Lighting Arnold Flames: Resonance in Doubly Forced Periodic Oscillators

Bruce B. Peckham†
Dept. of Mathematics and Statistics
University of Minnesota, Duluth
Duluth, Minnesota 55812
bpeckham@d.umn.edu

Ioannis G. Kevrekidis
Dept. of Chem. Engineering
Princeton University
Princeton, NJ 08544
yannis@arnold.princeton.edu

July 15, 2002

Abstract

We study doubly forced nonlinear planar oscillators:

$$\dot{\mathbf{x}} = \mathbf{V}(\mathbf{x}) + \alpha_1 \mathbf{W}_1(\mathbf{x}, \omega_1 t) + \alpha_2 \mathbf{W}_2(\mathbf{x}, \omega_2 t),$$

whose forcing frequencies have a fixed rational ratio: $\omega_1 = \frac{m}{n}\omega_2$. After some changes of parameter, we arrive at the form we study:

$$\dot{\mathbf{x}} = \mathbf{V}(\mathbf{x}) + \alpha\{(2-\gamma)\mathbf{W}_1(\mathbf{x}, \frac{m\,\omega_0}{\beta}t) + (\gamma-1)\mathbf{W}_2(\mathbf{x}, \frac{n\,\omega_0}{\beta}t)\}.$$

We assume $\dot{\mathbf{x}} = \mathbf{V}(\mathbf{x})$ has an attracting limit cycle — the unforced planar oscillator — with frequency ω_0, and the two forcing functions $\mathbf{W}_1$ and $\mathbf{W}_2$ are period one in their second variables. We consider two parameters as primary: β, an appropriate multiple of the forcing period, and α, the forcing amplitude. The relative forcing amplitude $\gamma \in [1, 2]$ is treated as an auxiliary parameter. The dynamics are studied by considering the stroboscopic maps induced by sampling the solutions of the differential equations at time intervals equal to the period of forcing, $T = \frac{\beta}{\omega_0}$. For any fixed γ, these oscillators have a standard form of a periodically forced oscillator, and thus exhibit the Arnold resonance tongues in the primary parameter plane. The special forms at $\gamma = 1$ and $\gamma = 2$ can introduce certain symmetries into the problem. One effect of these symmetries is to provide a relatively natural example of oscillators with multiple attractors. Such oscillators typically have interesting bifurcation features *within* corresponding resonance regions — features we call "Arnold flames" because of their flamelike appearance in the corresponding bifurcation diagrams. By changing the auxiliary parameter γ we "melt" one singly forced oscillator bifurcation diagram into another, and in the process we control certain of these "intraresonance region" bifurcation features.

Keywords: Periodically forced oscillators, Hopf bifurcation, resonance, resonance horns, resonance surfaces, Arnold tongues, Arnold flames, symmetry breaking

AMS Subject classification: 34C15, 34C25, 37E30, 37G40, 37G05

† Author to whom correspondence should be addressed.

1 Introduction

The motivation for the current bifurcation study originally comes from the setting of periodically forced nonlinear planar oscillators. Such systems arise in many contexts in science and engineering. Because the study of periodically forced oscillators usually involves a reduction to maps of the plane (see Section 2 below), results apply to the more general setting of bifurcations of families of maps of the plane.

The basic model we study in this paper has several equivalent forms:

$$\dot{\mathbf{x}} = \mathbf{V}(\mathbf{x}) + \alpha_1 \mathbf{W}_1(\mathbf{x}, \omega_1 t) + \alpha_2 \mathbf{W}_2(\mathbf{x}, \omega_2 t) \tag{1}$$

$$\dot{\mathbf{x}} = \mathbf{V}(\mathbf{x}) + \alpha\{(2-\gamma)\mathbf{W}_1(\mathbf{x}, m\,\omega\, t) + (\gamma-1)\mathbf{W}_2(\mathbf{x}, n\,\omega\, t)\} \tag{2}$$

$$\dot{\mathbf{x}} = \mathbf{V}(\mathbf{x}) + \alpha\{(2-\gamma)\mathbf{W}_1(\mathbf{x}, \frac{m\,\omega_0}{\beta} t) + (\gamma-1)\mathbf{W}_2(\mathbf{x}, \frac{n\,\omega_0}{\beta} t)\}. \tag{3}$$

$$\dot{\mathbf{x}} = \mathbf{V}(\mathbf{x}) + \alpha \widehat{\mathbf{W}}_\gamma(\mathbf{x}, \frac{\omega_0}{\beta} t) \tag{4}$$

The phase variable(s) $\mathbf{x} \in \mathcal{R}^2$, time $t \in \mathcal{R}$, and m and n are integers. When $\alpha = 0$ the corresponding autonomous differential equation is assumed to have an attracting limit cycle, the "unforced oscillator," whose (fixed) frequency we denote ω_0. The two forcing functions $\mathbf{W}_1$ and $\mathbf{W}_2$ are assumed to be periodic with period one in their second variables. We shall consider the form in eq. (3) as our primary doubly forced oscillator model. The parameter $\alpha \in [0, \infty)$ is the the forcing amplitude. We call the parameter $\beta \in (0, \infty)$ a "rotation parameter" for reasons that we will explain below. The parameter $\gamma \in [1, 2]$ is the relative forcing amplitude.

The parameters in equations (1), (2), and (3) are related as follows: $\omega_1 = m\omega = \frac{m\,\omega_0}{\beta}$, $\omega_2 = n\omega = \frac{n\,\omega_0}{\beta}$, $\alpha = \alpha_1 + \alpha_2$ (all three are nonnegative), $\gamma = 1 + \frac{\alpha_2}{\alpha_1+\alpha_2}$ (γ is arbitrary if $\alpha_1 = \alpha_2 = 0$). Equations (3) and (4) are seen to be equivalent by defining

$$\widehat{\mathbf{W}}_\gamma(\mathbf{x}, t) = (2-\gamma)\mathbf{W}_1(\mathbf{x}, m\, t) + (\gamma-1)\mathbf{W}_2(\mathbf{x}, n\, t). \tag{5}$$

We remark that if the ratio $\frac{\omega_1}{\omega_2}$ were fixed at an irrational number, this would instead be a model for a quasiperiodically forced oscillator. Such models are considered in, for example, in Glendinning et. al. [GFPS 2000]. See also earlier papers of Baesens, Guckenheimer, Kim and MacKay [BGKM 1991a, BGKM 1991b] for work on three frequency systems (including an oscillator with two periodic forcing terms). We do not consider quasiperiodic forcing here.

Motivated by previous studies of (singly) periodically forced oscillators, we choose to consider the rotation parameter β and the forcing amplitude α as primary parameters, and the relative forcing frequency γ as an auxiliary parameter. The unforced frequency ω_0 is assumed to be fixed. The main question we address

in this paper is how the traditional (β, α) parameter plane bifurcation diagram for $\gamma = 1$ "melts" into the corresponding parameter plane bifurcation diagram for $\gamma = 2$. The results, at least for the simplest nontrivial case $(m = 1, n = 2)$ are displayed in Figure 3. The primary features in these bifurcation diagrams are "resonance regions" — regions of the parameter plane for which the corresponding maps all have periodic orbits of a certain period (and rotation number). These resonance regions, which have a characteristic shape depending on the associated period, evolve from one characteristic shape into another. For example, the $\frac{1}{1}$ region melts from a triangular shape at $\gamma = 1$ (labelled $\mathbf{F}_{(1,\beta,\alpha)}$ in Fig. 3) to an ice cream cone shape at $\gamma = 2$ (labelled $\mathbf{F}_{(2,\beta,\alpha)}$ in Fig. 3). This evolution of resonance regions includes the creation of "extra" bifurcation features which we call "Arnold flames." A more complete description of Figure 3 and an explanation of the underlying mathematics is a major focus of this paper.

Note that if m and n are relatively prime and $\gamma \in (1, 2)$, $\widehat{\mathbf{W}}_\gamma(\mathbf{x}, t)$ in eq. (5) will have been normalized to be period one in its second variable; thus, $T = \frac{1}{\omega} = \frac{\beta}{\omega_0}$ is the forcing period. We will be studying the time T stroboscopic maps of the flow of eq. (3). When $\gamma = 1$, however, the time period of forcing is $\frac{T}{m}$, so the time T stroboscopic map is nongeneric because it is the m^{th} iterate of the time $\frac{T}{m}$ stroboscopic map. This "symmetry" of being the m^{th} iterate of a map (assuming $m > 1$) turns out to be exactly what we need to guarantee the existence of Arnold flames when γ is increased from 1. A similar phenomenon occurs for γ near 2 whenever $n > 1$. More details are provided later in the paper.

The rest of the paper is organized as follows. Section 2 includes a summary of relevant known results about singly forced oscillators, including the reduction to circle maps for small forcing amplitude, and "Arnold flames" created directly from circle maps. In Section 3 we perform a preliminary analysis of the doubly forced oscillators. This allows us to better explain the numerical results – essentially Fig. 3 – in Section 4. Part of the explanation involves looking at "resonance surfaces" which have been extremely useful in past work [MP 1994] in studying parameter plane resonance regions. We also describe the actual family we used for computations. It is a caricature of the model of eq. (3) which uses a more computationally efficient "impluse forcing" instead of periodic forcing in the form of eq. (3).

In Section 5, we present results of numerical computations from a doubly forced oscillator of the form of our model in eq. (3). In Section 6, we give a brief analysis of both the small forcing amplitude "lower tips" of the resonance regions, and the "upper tips" of the resonance regions near the Hopf bifurcation curve. We focus on how the bifurcation diagram near the tips evolves as the relative forcing amplitude γ is perturbed from 1 or from 2.

Software Remarks. All data for bifurcation curves and surfaces shown in the Figures in this paper were computed using the software To Be Continued [P 1988-

2001]. The regions for periods of 3 or higher in Fig. 3 were obtained by computing the whole corresponding resonance surface and then projecting it to the parameter plane, rather than by computing the saddle-node curves that project to the boundaries of these regions directly.

Computing the saddle-node curves in Fig. 6 required computation of the stroboscopic map linearization. This was done by integrating the variational and sensitivity equations for the original differential equation as in ODESSA [LK 1988].

Although not used directly, the authors acknowledge ideas and algorithms used in the continuation software package AUTO [Do 1981, DK 1986 and 1994, Tay 1990].

2 Background

2.1 Periodically Forced Oscillator Setting

A standard setting for studying periodically forced oscillators is the following:

$$\dot{\mathbf{x}} = \mathbf{V}(\mathbf{x}) + \alpha \mathbf{W}(\mathbf{x}, \omega t) \tag{6}$$

$$= \mathbf{V}(\mathbf{x}) + \alpha \mathbf{W}(\mathbf{x}, \frac{\omega_0}{\beta} t) \tag{7}$$

where the phase variable(s) $\mathbf{x} \in \mathcal{R}^2$, the forcing amplitude $\alpha \in [0, \infty)$, and the forcing frequency $\omega \in (0, \infty)$. When $\alpha = 0$ (the unforced oscillator) the corresponding autonomous differential equation is assumed to have an attracting limit cycle C with fixed frequency ω_0. For simplicity its basin of attraction is often assumed to be the whole plane, excepting a repelling equilibrium point inside the limit cycle. The forcing function $\mathbf{W}$ is assumed to be periodic – period one – in its second variable. Eq. (7) shows the effect of replacing the original forcing frequency parameter ω in eq. (6) with the "rotation parameter" β via $\beta = \frac{\omega_0}{\omega}$. Why β is called a rotation parameter is explained in subsection 2.2 below.

Thus eq. (6) represents a two-parameter family — parameters α and ω — of differential equations on the solid torus: $(x, t) \in \mathcal{R}^2 \times \mathcal{S}$. Similarly, eq. (7) represents a two-parameter family — parameters β and α (the unforced frequency ω_0 is assumed to be fixed) — of differential equations on the solid torus. These differential equations on the solid torus can be reduced to maps of the plane by stroboscopically sampling the respective flows at time intervals equal to the period of forcing, $T = \frac{1}{\omega} = \frac{\beta}{\omega_0}$. More precisely, let $\boldsymbol{\psi}_{(\beta,\alpha)}(\boldsymbol{\xi}, t)$ be the solution of the initial value problem $\dot{\mathbf{x}} = \mathbf{V}(\mathbf{x}) + \alpha \mathbf{W}(\mathbf{x}, \frac{\omega_0}{\beta} t), \quad \mathbf{x}(0) = \boldsymbol{\xi}$. The stroboscopic maps of the plane are defined by

$$\mathbf{F}_{(\beta,\alpha)}(\boldsymbol{\xi}) \equiv \boldsymbol{\psi}_{(\beta,\alpha)}(\boldsymbol{\xi}, \frac{\beta}{\omega_0}). \tag{8}$$

For each parameter value, the map $\mathbf{F}_{(\beta,\alpha)}$ is a diffeomorphism of the plane and is as smooth as the original equation (7), which, in this paper, is assumed to be C^∞.

2.2 Circle maps: small forcing amplitude

For small forcing amplitude, the state space can be further reduced because all the interesting dynamics lies on an attracting invariant circle which persists from the unforced limit cycle by assuming the limit cycle is normally hyperbolic. In this case, the reduction leaves us with a two-parameter family of circle maps. Note that at $\alpha = 0$, the corresponding circle map is just the time $T = \frac{1}{\omega} = \frac{\beta}{\omega_0}$ map of the autonomous flow of $\dot{\mathbf{x}} = \mathbf{V}(\mathbf{x})$. The attracting limit cycle of the autonomous flow becomes an attracting invariant circle for the corresponding stroboscopic maps, and especially when the original limit cycle is assumed to be globally attracting (except for the repelling equilibrium for the autonomous flow which becomes a repelling fixed point for the stroboscopic maps), all the important dynamics for the stroboscopic maps will "live" on the invariant circles. As the forcing amplitude α is increased away from zero, the invariant circles, assuming they were normally hyperbolic at $\alpha = 0$, persist. Thus, the study of periodically forced oscillators can be reduced to the study of circle maps, at least for small forcing amplitude.

Arnold tongue resonance regions. The stroboscopic maps $\mathbf{F}_{(\beta,\alpha)}$ restricted to the continuation of the invariant circle from the limit cycle C, and lifted to the real line, have the form

$$\tilde{F}_{(\beta,\alpha)}(u) = u + 2\pi\beta + \alpha g_{(\beta,\alpha)}(u) \tag{9}$$

where $u \in \mathcal{R}$ and $g_{(\beta,\alpha)}$ is period 2π in u. Note that since the circle maps are one-dimensional, we have dropped the boldface for the maps, and because it is a lift, we have added the tilde. This form can be understood by returning to eq. (7) and fixing the first primary parameter α at zero. We see that, since the stroboscobic maps are defined as the time $\frac{\beta}{\omega_0}$ map of the autonomous flow, they are conjugate to a rigid rotation with rotation number β. Thus the lifted circle maps derived from eq. (7) are conjugate to maps in the form of eq. (9).

The most famous map in the form of eq. (9) is the Arnold Standard Circle Map Family for which the forcing function $g_{(\beta,\alpha)}(u) = \sin(u)$. It is in this circle map setting where wedge-shaped resonance regions — also called Arnold tongues or resonance horns — are generically shown to open up from each rational point on the β axis into the upper half of the parameter plane [Ar 1965, Ha 1984]. A portion of the now familiar Arnold tongue picture for the Standard Family is shown in the (β, α) parameter plane in Fig. 1 (reproduced from [MP 1996]). The "complete" small α bifurcation picture would require a resonance tongue emanating from each rational β value on the $\alpha = 0$ axis. This Arnold tongue

picture is also the start of the bifurcation diagram for the periodically forced oscillator maps – for small forcing amplitude. Compare the small α part of the bifurcation diagrams in Fig. 3 with the (β, α) resonance regions in Fig. 1.

Resonance surfaces. Also illustrated in Fig. 1 are p/q surfaces which live in the Cartesian product of the (lifted) phase variable u (where $\theta = u \bmod(2\pi)$) and parameter variables β and α, and project to the parameter plane tongues. The surfaces are defined as follows. First define a ***p/q* resonance point** as a least-period-q point which satisfies $\tilde{F}^q_{(\beta,\alpha)}(u) = u + 2\pi p/q$. The ***p/q* resonance surface**, denoted $\Gamma^{p/q}$, is then defined as

$$\Gamma^{p/q} = \{(u, \beta, \alpha) : u \text{ is a } p/q \text{ resonance point for } \tilde{F}^q_{(\beta,\alpha)}\}. \tag{10}$$

For example, from eq. (9), the 0/1 resonance surface in the figure is defined by $2\pi\beta + \alpha g_{(\beta,\alpha)}(u) = 0$. Viewing the $\frac{p}{q}$ resonance region as a projection of the $\frac{p}{q}$ resonance surface makes more obvious the appearance of the regions: the tip of the region (tongue) is merely an artifact of the projection to the parameter plane, and the saddle-node bifurcation curves that make up the boundary of the resonance region in the parameter plane are merely the singularities of the resonance surface with respect to projection of the surface to the parameter plane. That is, the saddle-nodes are the folds in the resonance surfaces. The $\frac{p}{q}$ resonance region itself is the set of parameter values for which the corresponding map has a period-q point with rotation number $\frac{p}{q}$.

2.3 Periodically forced oscillator maps: beyond small forcing amplitude

In order to analyze behavior at higher forcing amplitudes, circle maps are no longer adequate. This is because the invariant circles which are guaranteed to persist for small values of α may (and typically do) "break" for higher values of α. It is therefore necessary to revert to studying either the full flow of eq. (7) or the associated stroboscopic maps of the plane $\mathbf{F}_{(\beta,\alpha)}$ defined in eq. (8).

Continuation from small forcing amplitude and closing of resonance regions. The breakdown of the invariant circles, however, does not affect the existence of the periodic orbits which originally (for small forcing amplitude) lived on the circles. In particular, the saddle-node curves whose projection to the parameter plane determined the boundaries of the Arnold tongues for small forcing amplitude (see Fig. 1) can be numerically continued in a straightforward manner to higher forcing amplitude α. The notion of a resonance region in the parameter plane, except for the period-one case, also generalizes from the circle map to the planar map setting. Fixed-point regions differ because a fixed point exists for all

parameter values; this omnipresent fixed point can be thought of as the continuation of the repelling fixed point corresponding to the repelling equilibrium point inside the original unforced oscillator limit cycle. Consequently, we will use the term "fixed-point resonance region" to denote a region where the corresponding maps have more than one fixed point. The saddle-node continuation for many different examples [KT 1979, KAS 1986, AMKA 1986, SDCM 1988, VR 1989, P 1990, MP 1995] suggests all resonance regions for periods greater than one eventually "close" when the forcing amplitude α becomes sufficiently large.

This resonance region "closing" for forced oscillators is quite different from the high forcing amplitude behavior for the circle maps of the form of eq. (9), whose periodic orbits persist for arbitrarily large values of the forcing amplitude α. In the context of the corresponding stroboscopic maps, this means that for high enough forcing, the maps have a globally attracting fixed point; any other resonance behavior must have terminated at some lower forcing amplitude. The assumption that this observation is true, specifically that the components of sets of periodic points other than fixed points are bounded in the four-dimensional cartesian product of phase and parameter spaces, is sufficient to prove that resonance regions generically "terminate" with a Hopf bifurcation [P 1990]. This explains the prominence of the (high α) Hopf bifurcation curve in periodically forced oscillator bifurcation diagrams. Typical such bifurcation diagrams, with only a few of the resonance regions shown, are the diagrams in Fig. 3 which are labelled by $\mathbf{f}_{(1,\beta_1,\alpha)}$ and $\mathbf{f}_{(2,\beta_2,\alpha)}$.

The shape of a typical period-q resonance region. Although generic resonance regions for all periods (even including period one) "open" (at low forcing amplitude) in a qualitatively similar wedge, they "close" (at the Hopf bifurcation) in a manner that varies greatly, depending on the associated period. The differences are largely explained by, or at least consistent with, the normal forms theory associated with $\boldsymbol{\frac{p}{q}}$ **resonant Hopf bifurcations**: Hopf bifucations with an additional requirement that the eigenvalues at the bifurcation are $e^{\pm 2\pi i \frac{p}{q}}$ [Ar 1977, Ar 1983, Bo 1976, Ta 1974]. The normal forms theory guarantees that, generically, all resonance regions for periods of five or greater, classified as weak resonance cases, will close in a cusp.

In the strong resonance cases ($q \leq 4$), resonance region "closing" depends on the period. More specifically, period-one resonance regions typically have two "upper" cusps near the Hopf bifurcation curve, giving the period-one saddle-node set a triangular shape. Period-two regions close with period-two saddle-nodes connecting with a period-doubling circle, giving the full period-two region an ice cream cone shape. Period-three regions close with a rounded top; the full period-three region thus has an inverted teardrop shape. Period-four resonance regions can close either with a rounded top like period-three horns or with a tip like period-five horns. These strong resonance closing phenomena are all consistent

with the numerical studies referred to above as well as the local analysis of Arnold [Ar 1977] and Takens [Ta 1974]. See also Baesens [Ba 1987] and Gambaudo [Ga 1985] for work related to resonance region closings. There are, of course, variations on these basic phenomena, but the point is that the period of a resonance region is usually easy to deduce from its shape (all periods ≥ 5 being grouped together).

2.3.1 Resonance surfaces

Just as the resonance regions for circle maps are better understood as projections to the parameter plane of resonance surfaces in the phase $\times$ parameter space (Fig. 1), so also are these resonance regions for the periodically forced oscillator maps better understood in the same manner. For $q \geq 2$, a $\frac{p}{q}$ resonance surface is defined analogously to a $\frac{p}{q}$ resonance surface for the circle maps (eq. (10)), but the definition is more involved. We first define the **least-period-q surface** $\Gamma(q)$ as

$$\Gamma(q) = \{(\mathbf{x}, \beta, \alpha) : \mathbf{x} \text{ is a least} - \text{period}{-}q \text{ point for } \mathbf{F}^q_{(\beta,\alpha)}\}. \tag{11}$$

Next we define $\Gamma^{p/q}$ as the connected component of $\Gamma(q)$ which includes $C \times \{\frac{p}{q}\} \times \{0\}$ (recall that C was the unforced oscillator in the phase space). Finally, we can define the $\boldsymbol{\frac{p}{q}}$ **resonance surface** as

$$\overline{\Gamma^{p/q}} \equiv \text{the topological closure of } \Gamma^{p/q}. \tag{12}$$

The $\boldsymbol{\frac{p}{q}}$ **resonance region** is then defined to be the projection to the parameter plane of the $\frac{p}{q}$ resonance surface. It can be shown, using a generalization of the rotation number for circle maps to self rotation number for maps of the plane [P 1990], that, if $q \geq 2$, all points on a $\frac{p}{q}$ resonance surface have self rotation number $\frac{p}{q}$. Consequently, there is a distinct p/q resonance surface for each distinct p/q with $q \geq 2$. The fixed-point surface does not have this "constant rotation number" property, so a $p_1/1$ surface and a $p_2/1$ surface could actually be the same surface. In fact, the families we have studied have a single component of the fixed-point surface: the continuation of the fixed-point surface from each unforced oscillator $C \times \{\frac{j}{1}\}, \times\{0\}$ for each integer j connects with the continuation of the part of the fixed point surface corresponding to the repelling fixed point inside the unforced oscillator. Consequently, we define a $\frac{j}{1}$ **resonance region** as the region of the (β, α) parameter plane which corresponds to maps having more than one fixed point and includes the point $(\frac{j}{1}, 0)$.

Displaying a $\frac{p}{q}$ resonance surface and its projection to a $\frac{p}{q}$ resonance region is more complicated than in the circle map setting of Fig. 1: the phase $\times$ parameter space is now four-dimensional. It is still, however, more informative than merely displaying the resonance regions themselves. This was performed and explained in detail for a specific family in previous work [MP 1994]. In that paper, we numerically verified that the $\frac{1}{5}$ surface is a topological disk in the four-dimensional

phase × parameter space. The topological disk is most obvious in a projection to a three-dimensional space which includes the phase plane.

Since we are more interested in this paper in the projection to the parameter plane, prefer a projection from four to three dimensions which includes the parameter plane. Unfortunately, choosing either one of the phase variables as the third variable leads to false self intersections due only to the projection from four to three dimensions. We can, however, show a projection to the parameter plane and one phase variable which has no self intersections by displaying only a "fundamental sector" of the $\frac{1}{5}$ surface. That is, we display a sector on which each $\frac{1}{5}$ *orbit* is represented. We do so schematically in Fig. 5. The lowest of the four surfaces ($\gamma = 1$) can be thought of as the singly forced oscillator representative. The front and back edges of the surface are identified because corresponding points lie on the same period-5 orbit. This turns the surface into a topological cone. The boundary of the cone is the unforced oscillator at $\alpha = 0$. The tip of the cone is a $\frac{1}{5}$ resonant Hopf bifurcation point. The saddle-node bifurcation curves are seen to project to the boundaries of the $\frac{1}{5}$ resonance region. To compare this surface with the resonance surfaces for the circle maps in Fig. 1, we would need to identify the top edge of each surface in Fig. 1 to a point. This is analogous to the oversimplified, but still useful, idea that the circle on which the circle maps are defined shrinks to a point at $\alpha = 1$; the $\frac{1}{5}$ orbits for the forced oscillators collapse to a fixed point at a Hopf bifurcation point.

The typical picture for any resonance surface of period five or greater is similar. The surfaces for the strong resonance cases, however, are more difficult to describe. See McGehee and Peckham [MP 1994] for more details.

2.4 Arnold flames for circle maps.

We now return briefly to the circle map setting of eq. (9). We also restrict α to be small enough so that the corresponding maps are diffeomorphisms. For the Standard Family, this means $\alpha < 1$. For general circle maps with lifts of the form of eq. (9), the division of the circle map parameter plane into resonance regions is not necessarily the complete bifurcation story. For some families (but not for the Standard Family) it is possible for some maps inside the same resonance region to be topologically non-equivalent. The easiest way for such maps to be non-equivalent is for one map to have a single pair of attracting-repelling periodic orbits, and another to have two such pairs. Saddle-node bifurcation curves would typically divide the resonance region into subregions. The number of periodic orbits of the given period would be the same in each subregion. Fourier series analysis shows that these extra orbits can be created by adjusting the relative magnitudes of certain Fourier coefficients in the Fourier series for the forcing function $g_{(\beta,\alpha)}(\theta)$.

This simple observation led to the construction of a multitude of bifurcation

features interior to resonance regions: swallowtails, flames, and interchanging of curve segments which marked the boundary of resonance regions [MP 1996]. One such bifurcation diagram, called a "single flame," is shown in Fig. 2. Note that for parameter values inside the flame there are four fixed points, while for parameter values outside the flame but inside the tongue, there are two fixed points. The saddle-nodes corresponding to the flame form a smooth boundary in the full phase $\times$ parameter space, but project to the parameter plane with a cusp which is the upper tip of the flame.

2.5 Arnold flames for periodically forced oscillator maps.

We emphasize that the examples in McGehee and Peckham [MP 1996] were all created by manipulating Fourier series in the circle map setting. By reversing the reduction process mentioned above: flows on the solid torus to maps of the plane to circle maps, the circle map phenomena presented were known to be possible for periodically forced oscillators, as well.

The connection between the original differential equations (eq. (7)) and the Fourier series coefficients for the corresponding circle map, however, is not so obvious. This paper extends the understanding of intraresonance region phenomena from circle maps to periodically forced oscillator maps in two significant ways. The first is that we work in this paper directly with the periodically forced oscillator (equation (7) or (3)) rather than with the Fourier series of the reduced circle maps. The second is that extra orbits are created in parts of resonance regions "far away" from the zero forcing amplitude. Since the invariant circles are guaranteed to exist only for small forcing amplitude, the regions of parameter space considered in this paper cannot be treated by reducing to circle maps. For such parameter values the Fourier series techniques of McGehee and Peckham [MP 1996], which assume the existence of a circle map, are not directly applicable. Doubly forced oscillators also provide a natural setting in which intraresonance region bifurcation features not only occur, but also can be created and somewhat controlled directly from the differential equations.

See also Broer, Simó and Tatjer [BST 1998] for a study of a wealth of dynamcal phenomena, including intraresonance region bifurcation features, for a family of maps of the annulus they call the "fattened Arnold family."

3 Doubly Forced Oscillators

3.1 Preliminary analysis

We now return to the analysis of the doubly forced oscillator, copied from eq. (3) in the introduction:

$$\dot{\mathbf{x}} = \mathbf{V}(\mathbf{x}) + \alpha\{(2-\gamma)\mathbf{W}_1(\mathbf{x}, \frac{m\,\omega_0}{\beta}t) + (\gamma-1)\mathbf{W}_2(\mathbf{x}, \frac{n\,\omega_0}{\beta}t)\}.$$

Notation. Following the notation introduced in Section 2, we let $\Psi_{(\gamma,\beta,\alpha)}(\boldsymbol{\xi}, t)$ be the flow of eq. (3) satisfying the initial condition $\mathbf{x}(0) = \boldsymbol{\xi}$. That is, $\Psi_{(\gamma,\beta,\alpha)}(\boldsymbol{\xi}, 0) = \boldsymbol{\xi}$. Note that, if m and n are relatively prime, since $\mathbf{W}_1$ and $\mathbf{W}_2$ were assumed to be period one in their second variable, the time period of forcing for $\gamma \in (1,2)$ is $\frac{\beta}{\omega_0}$, but for $\gamma = 1$ it is $\frac{\beta}{m\,\omega_0}$ and for $\gamma = 2$ it is $\frac{\beta}{n\,\omega_0}$. Consequently we introduce parameters $\beta_1 = \frac{\beta}{m}$ and $\beta_2 = \frac{\beta}{n}$ and define the following stroboscopic maps:

$$\mathbf{F}_{(\gamma,\beta,\alpha)}(x) = \Psi_{(\gamma,\beta,\alpha)}(\mathbf{x}, \frac{\beta}{\omega_0}),\ \gamma \in [1,2], \tag{13}$$

$$\mathbf{f}_{(1,\beta_1,\alpha)}(\mathbf{x}) = \Psi_{(1,m\beta_1,\alpha)}(\mathbf{x}, \frac{\beta_1}{\omega_0}) = \Psi_{(1,\beta,\alpha)}(\mathbf{x}, \frac{\beta}{m\omega_0}), \tag{14}$$

$$\mathbf{f}_{(2,\beta_2,\alpha)}(\mathbf{x}) = \Psi_{(2,n\beta_2,\alpha)}(\mathbf{x}, \frac{\beta_2}{\omega_0}) = \Psi_{(2,\beta,\alpha)}(\mathbf{x}, \frac{\beta}{n\omega_0}). \tag{15}$$

The maps $\mathbf{f}_{(1,\beta_1,\alpha)}$ and $\mathbf{f}_{(2,\beta_2,\alpha)}$ are "merely" singly forced oscillators and as such constitute the "well known" part of our bifurcation scenario. More specifically, the two-parameter bifurcation diagrams for $\mathbf{f}_{(1,\beta,\alpha)}$ and $\mathbf{f}_{(2,\beta,\alpha)}$ in Fig. 3 are relatively well understood.

The parameters β, β_1, and β_2 are defined so that they are the rotation numbers of $\mathbf{F}_{(\gamma,\beta,0)}$, $\mathbf{f}_{(1,\beta_1,0)}$, and $\mathbf{f}_{(2,\beta_2,0)}$, respectively, when restricted to their invariant circles. Thus we think of β (β_1, β_2, resp.) as rotation parameters, even though the rotation number of corresponding maps is guaranteed to match the rotation parameter only for zero forcing amplitude. In general, we will use no subscript when discussing variables associated with $\mathbf{F}_{(\gamma,\beta,\alpha)}$, subscript 1 when discussing variables associated with $\mathbf{f}_{(1,\beta_1,\alpha)}$, and subscript 2 when discussing quantities associated with $\mathbf{f}_{(2,\beta_2,\alpha)}$, We will be most interested in periodic orbits for the respective maps; their periods will be denoted q, q_1 and q_2; their rotation numbers will be denoted $\frac{p}{q}$, $\frac{p_1}{q_1}$, and $\frac{p_2}{q_2}$, respectively.

The main question can now be restated: "How do the bifurcation diagrams for $\mathbf{F}_{(\gamma,\beta,\alpha)}$ change as γ is varied?" As we shall see in the next sections, an oversimplified answer is that the bifurcation diagram for $\mathbf{F}_{(\gamma,\beta,\alpha)}$ "melts" from the bifurcation diagram for $\mathbf{f}_{(1,\beta_1,\alpha)}$ into the bifurcation diagram for $\mathbf{f}_{(2,\beta_2,\alpha)}$ as γ increases from one to two. The same is true for the corresponding resonance surfaces. What makes this melt interesting is that a $\frac{p_1}{q_1} = \frac{p}{mq}$ region for $\mathbf{f}_{(1,\beta_0,\alpha)}$ melts into a $\frac{p_2}{q_2} = \frac{p}{nq}$ region for $\mathbf{f}_{(2,\beta_1,\alpha)}$ via a $\frac{p}{q}$ region for $\mathbf{F}_{(\gamma,\beta,\alpha)}$. Note that while the period of a $\frac{p}{q}$ region is q, the period of a $\frac{p}{mq}$ region or a $\frac{p}{nq}$ region is the respective denominator only after cancelling any common factors between p and m (p and n, respectively). This melt is most interesting when the periods of the $\frac{p}{mq}$, $\frac{p}{q}$, and $\frac{p}{nq}$ regions are not all the same — even more so when any of the periods is less than five. This is explained more fully below.

Symmetry breaking near extreme values of γ: $\gamma = 1$ and $\gamma = 2$. We will first consider the simplest nontrivial example: $m = 1$ and $n = 2$. That is, the doubly forced oscillator of eq. (3) has the more specific form:

$$\dot{\mathbf{x}} = \mathbf{V}(\mathbf{x}) + \alpha\{(2-\gamma)\mathbf{W}_1(\mathbf{x}, \frac{1\,\omega_0}{\beta}t) + (\gamma-1)\mathbf{W}_2(\mathbf{x}, \frac{2\,\omega_0}{\beta}t)\}.$$

Since $m = 1$, there is no symmetry breaking near $\gamma = 1$, but since $n > 1$, there is a symmetry breaking as γ is perturbed away from $\gamma = 2$. So we will focus on γ near 2. From the definitions of the stoboscopic maps $\mathbf{F}_{(2,\beta,\alpha)}$ and $\mathbf{f}_{(2,\beta_2,\alpha)}$ in eqs. (13) and (15), and the definition of β_2 as $\beta_2 = \beta/2$, it can be seen that $\mathbf{F}_{(2,2\beta_2,\alpha)} = \mathbf{f}^2_{(2,\beta_2,\alpha)}$. This clearly makes the rotation number of $\mathbf{F}_{(2,2\beta_2,\alpha)}$ equal to twice the rotation number of $\mathbf{f}_{(2,\beta_2,\alpha)}$. This also causes the period of any periodic orbit with an even period q_2 for $\mathbf{f}_{(2,\beta_2,\alpha)}$ to have period $q = q_2/2$ for $\mathbf{F}_{(2,2\beta_2,\alpha)}$. A point with odd period for $\mathbf{f}_{(2,\beta_2,\alpha)}$, however, will still have the same period for its second iterate, $\mathbf{F}_{(2,2\beta_2,\alpha)}$. We combine these two cases by saying that a period-q_2 point for $\mathbf{f}_{(2,\beta_2,\alpha)}$ is a period-$\frac{q_2}{\gcd(2,q_2)}$ point for $\mathbf{F}_{(2,2\beta_2,\alpha)}$. The consequence is that the two-parameter bifurcation diagrams: in (β_2, α) for $\mathbf{f}_{(2,\beta_2,\alpha)}$ and in (β, α) for $\mathbf{F}_{(2,\beta,\alpha)}$), are identical. One needs only make the correspondences just stated: β corresponds to $2\beta_2$, and period-q coresponds to period-$\frac{q_2}{\gcd(2,q_2))}$. See the labelling in Fig. 3.

The "symmetry" of being a second iterate of another map at $\gamma = 2$ forces "extra" orbits in the resonance regions for $\mathbf{F}_{(2,2\beta_2,\alpha)}$ corresponding to even periods for $\mathbf{f}_{(2,\beta_2,\alpha)}$. This in turn leads to the existence of "flames" in the bifurcation diagram for $\mathbf{F}_{(\gamma,\beta,\alpha)}$ when γ is sufficiently close to 2. To explain this phenomenon, let us first assume that the parameter plane bifurcation diagram for $\mathbf{f}_{(2,\beta_2,\alpha)}$ is both "typical" and "simple." Being typical means we assume that its resonance regions all appear as one would expect: triangles for period-one regions, ice cream cones for period-two regions, inverted teardrops for period-three regions, and points (cusps or wedges) at the top and bottom for period-five and higher regions. Being simple means the maps in any $\frac{p_2}{q_2}$ resonance region all have the minimum number of period-q_2 orbits. For weak resonances ($q_2 \geq 5$), this means there exist exactly two period-q_2 orbits on the interior of the $\frac{p_2}{q_2}$ region; they coalesce to a single saddle-node orbit for parameter values on the boundary of the $\frac{p_2}{q_2}$ region. For strong resonances ($q_2 \leq 4$), the analogous statement is more difficult to make. The exceptions to the "exactly two orbit" condition are as follows. Period-4 regions may and period-3 regions generically do have a single interior parameter value (the resonant Hopf bifurcation point) where one of the two periodic orbits coalesces to a fixed point. Period-2 regions have subregions (inside the period-doubling circle) where only one of the two orbits still persists. Recall that period-1 regions are complicated by the continuation of the fixed point corresponding to the repelling equilibrium of the unforced oscillator. Thus, we will call a fixed point region simple if it has three fixed points for parameter values in its interior

(including one fixed point which continues to parameter values outside it).

As a consequence of our "typical and simple" assumptions, there are no period-q_2 saddle-node curves *interior* to any $\frac{p_2}{q_2}$ region. That is, the resonance regions have no flames. The resonance regions shown for $\mathbf{f}_{(2,\beta_2,\alpha)}$ in Fig. 3 are all typical and simple. Consider, for example, the $\frac{1}{4}$ resonance region in the (β_2, α) bifurcation diagram for $\mathbf{f}_{(2,\beta_2,\alpha)}$ in Fig. 3. Being typical and simple, it has exactly two period-4 orbits, and therefore exactly 8 period-4 points, for every parameter value on the interior of the resonance region. In the bifurcation diagram for its second iterate, $\mathbf{F}_{(2,\beta,\alpha)}$, the 2 period-4 orbits with rotation number $\frac{1}{4}$ turn into 4 period-2 orbits with rotation number $\frac{1}{2}$. Thus $\mathbf{f}_{(2,\beta_2,\alpha)}$ has an extra pair of rotation number $\frac{1}{2}$ orbits. By continuity, the extra orbits will persist at least for some parameter values in the interior of the $\frac{1}{2}$ region as γ is decreased from 2. On the other hand, since the bifurcation diagram for $\mathbf{F}_{(1,\beta,\alpha)}$ is exactly the same as the typical and simple bifurcation diagram for $\mathbf{f}_{(1,\beta_1,\alpha)}$, it cannot have the extra two period-2 orbits that $\mathbf{F}_{(2,\beta,\alpha)}$ has. So, the extra orbits must disappear as γ decreases from 2 to 1. This combination guarantees that the bifurcation diagrams for $\mathbf{F}_{(\gamma,\beta,\alpha)}$ must have intraresonance bifurcation curves in its $\frac{1}{2}$ resonance regions, at least for $\gamma \in (2-\delta, 2)$, for some $\delta > 0$. The evolution of $\frac{1}{2}$ intraresonance region is partially illustrated in Fig. 3. See especially the flame in the enlargement in Fig. 4. Further explanation follows in subsection 4.2.

Remark: The $\frac{1}{2}$ region for $\mathbf{f}_{(1,\beta_1,\alpha)}$ in Fig. 3 has a slight complication which prevents it from being simple: the upper right-hand side of the cone extends into the ice cream. The complication is not atypical or degenerate, merely not the simplest possible case. It is of special interest to the authors because it implies the existence of a codimension-three bifurcation point – a period-doubling with two higher order degeneracies [PK 1991] for some γ between 1.7 and 1.0.

General values of m and n. Guided by the special case of $m = 1$ and $n = 2$ explained above, we now state the analogous results for general values of m and n. The symmetries at the $\gamma = 1$ and $\gamma = 2$ endpoints are due to the fact that $\mathbf{F}_{(1,\beta,\alpha)} = \mathbf{f}^m_{(1,\beta/m,\alpha)}$ and $\mathbf{F}_{(2,\beta,\alpha)} = \mathbf{f}^n_{(2,\beta/n,\alpha)}$. Thus, the rotation number for any orbit under $\mathbf{F}_{(1,\beta,\alpha)}$ is m times the rotation number for the corresponding orbit under $\mathbf{f}_{(1,\frac{\beta}{m},\alpha)}$, so the (β, α) bifurcation diagram for $\mathbf{F}_{(1,\beta,\alpha)}$ is identical to the (β_1, α) bifurcation diagram for $\mathbf{f}_{(1,\beta,\alpha)}$, except for the parameter change $\beta = m\beta_1$. Period-q_1 points with rotation number $\frac{p_1}{q_1}$ for $\mathbf{f}_{(1,\beta_1,\alpha)}$ become for $\mathbf{F}_{(1,m\beta_1,\alpha)}$ period-q points ($q = \frac{q_1}{\gcd(m,q_1)}$) with rotation number $\frac{p}{q}$ (p chosen so that $\frac{p}{q} = m\frac{p_1}{q_1}$). The symmetries at $\gamma = 1$ will force $\frac{p}{q}$ regions for $\mathbf{F}_{(1,\beta,\alpha)}$ to have $\gcd(m, q_1)$ total pairs of $\frac{p}{q}$ orbits ($\gcd(m, q_1) - 1$ extra pairs of orbits). These extra orbits will lead to intraresonance regions features in the $\frac{p}{q}$ region for γ sufficiently close to 1.

Similarly, the rotation numbers for $\mathbf{F}_{(2,\beta,\alpha)}$ are all n times the corresponding

rotation numbers for $\mathbf{f}_{(2,\frac{\beta}{n},\alpha)}$, so the (β,α) bifurcation diagram for $\mathbf{F}_{(2,\beta,\alpha)}$ is identical to the (β_2,α) bifurcation diagram for $\mathbf{f}_{(2,\beta,\alpha)}$, except for the parameter change $\beta = n\beta_2$. Period-q_2 points with rotation number $\frac{p_2}{q_2}$ for $\mathbf{f}_{(2,\beta,\alpha)}$ become for $\mathbf{F}_{(2,n\beta_2,\alpha)}$ period-q points ($q = \frac{q_2}{\gcd(n,q_2)}$) with rotation number $\frac{p}{q}$ (p chosen so that $\frac{p}{q} = n\frac{p_2}{q_2}$). The symmetries at $\gamma = 2$ will force $\frac{p}{q}$ regions for $\mathbf{F}_{(2,\beta,\alpha)}$ to have $\gcd(n,q_2)$ total pairs of $\frac{p}{q}$ orbits ($\gcd(n,q_2)-1$ extra pairs of orbits). These extra orbits will be lead to intraresonance region features in the $\frac{p}{q}$ region for γ sufficiently close to 2.

In summary, we see that a $\frac{p}{q}$ resonance region for $\mathbf{F}_{(\gamma,\beta,\alpha)}$ melts from a period-q_1 shape into a period-q_2 shape as γ increases from 1 to 2. In the process of this transformation, intraresonance region features – flames – will exist near $\gamma = 1$ whenever $\gcd(m,q_1) > 1$, and near $\gamma = 2$ whenever $\gcd(n,q_2) > 1$. Assuming that the parameter plane bifurcation diagrams for $\mathbf{f}_{(1,\beta_1,\alpha)}$ and $\mathbf{f}_{(2,\beta_2,\alpha)}$ are both "typical" and "simple," the number of flames for γ near 1 will be $\gcd(m,q_1)-1$, and the number of flames for γ near 2 will be $\gcd(n,q_2)-1$. Further explanation of the evolution of the flames is included in Sections 4 and 6.

4 Numerical results

We now present the numerical results which illuminate and corroborate many of the ideas presented in the previous sections. In later sections we will return to the analysis, especially to study the behavior at the zero forcing tips of resonance regions, and at the Hopf bifurcation curve where the resonance regions close.

We first describe the actual maps on which we performed our numerical study.

4.1 DFO Caricature

Because of the computational effort necessary in numerically integrating the differential equations in the form of eq. (3), and because of the lack of explicit derivatives, we have done the majority of our numerical work instead on a caricature of a doubly forced oscillator. The main goal in constructing the caricature is to directly obtain a family of maps which has the properties of the stroboscopic maps which were defined as the the time-$\frac{1}{\omega}$ (recall $\frac{1}{\omega} = \frac{\beta}{\omega_0}$) maps of the differential equations of eq. (3).

Periodically forced oscillator caricature. Since the doubly forced oscillator caricature, labelled $\mathbf{F}_{(\gamma,\beta,\alpha)}$ below, is a generalization of an "impulse forcing" caricature previously used [P 1990, MP 1994, MP 1995, P 2000] for singly forced oscillators, we begin with a short review of the singly forced caricature, labelled $\widehat{\mathbf{F}}_{(\beta,\alpha)}$, taken from McGehee and Peckham [MP 1994]. More details are included in that reference.

We define the family of maps $\widehat{\mathbf{F}}_{(\beta,\alpha)}$ by the composition

$$\widehat{\mathbf{F}}_{(\beta,\alpha)} \equiv \mathbf{g}_\alpha \circ \mathbf{h}_{\beta,1}$$

where the two maps $\mathbf{g}_\alpha$ and $\mathbf{h}_{\beta,t}$ are defined as follows. For $\beta \in \mathcal{R}$, the map $\mathbf{h}_{\beta,t}$ is taken to be the time t flow of the following planar vector field, written here in polar coordinates.

$$\begin{aligned} \dot{r} &= k\frac{r(1-r^2)}{1+r^2}, \\ \dot{\theta} &= 2\pi\beta + \frac{1-r^2}{1+r^2}. \end{aligned} \tag{16}$$

For $\alpha \in [0,1)$, the map $\mathbf{g}_\alpha$ is defined by

$$\mathbf{g}_\alpha(\mathbf{z}) = (1-\alpha)(\mathbf{z}-1)+1.$$

where $\mathbf{z}$ is a complex number used as a coordinate on $\mathcal{R}^2$. Note that $\mathbf{g}_0$ is the identity map, while, for $0 < \alpha < 1$, the map $\mathbf{g}_\alpha$ is a linear contraction toward $\mathbf{z} = 1$. This type of caricature is often labelled a periodically forced oscillator with *impulse* forcing. The flow of the vector field is given a "kick" or "impulse" every "second" (once every unit of dimensionless time).

The form of eq. (16) has been chosen primarily to have two properties. First, it has an explicit analytic solution, which allows efficient computation of $\mathbf{h}_{\beta,t}$. Second, it has the unit circle as an attracting limit cycle, which constitutes the unforced oscillator. The function $\mathbf{h}_{\beta,1}$, and therefore also $\widehat{\mathbf{F}}_{(\beta,0)}$, being the time one flow of eq. (16), will have the unit circle as an attracting invariant circle on which the map is a rigid rotation with rotation number β. For small but positive α, an attracting invariant circle for $\widehat{\mathbf{F}}_{(\beta,\alpha)}$ persists, but it is distorted from the original unit circle. For α close to 1, the invariant circle and, indeed, all periodic orbits, have disappeared and there remains only an attracting fixed point near $z = 1$.

The function $\mathbf{g}_\alpha$ is the forcing function; α is the forcing amplitude. Using the time 1 flow of eq. (16) to define $\mathbf{h}_{\beta,1}$ is analogous to fixing the forcing frequency at one. Note that in experimental situations, the rotation parameter β, defined above as $\beta = \frac{\omega_0}{\omega}$, is usually controlled by varying the forcing frequency ω, which would have resulted in using $\mathbf{h}_{\beta,\frac{1}{\omega}}$ instead of $\mathbf{h}_{\beta,1}$. We choose instead to fix the forcing frequency ω at one, which makes $\omega_0 = \beta$. In other words, we control the rotation parameter β by varying the unforced oscillator frequency ω_0 instead of the forcing frequency ω. This parameter selection has the advantage that, restricted to its invariant circle, the maps have the circle map form of eq. (9).

Doubly forced oscillator caricature. It is now only a slight modification to obtain a caricature for a doubly forced oscillator from the forced oscillator caricature just described. We merely "kick" the oscillator at two different frequencies.

Each frequency has its own amplitude associated with it. For the simple case with $m = 1$ and $n = 2$, the caricature takes the form:

$$\mathbf{F}_{(\gamma,\beta,\alpha)} \equiv \mathbf{g}_{\alpha_2} \circ \mathbf{g}_{\alpha_1} \circ \mathbf{h}_{\beta,\frac{1}{2}} \circ \mathbf{g}_{\alpha_2} \circ \mathbf{h}_{\beta,\frac{1}{2}}, \tag{17}$$

where $\alpha_1 = \alpha(2-\gamma)$, $\alpha_2 = \alpha(\gamma-1)$, and $\gamma \in [1,2]$. To be consistent with the notation we already used for the doubly forced oscillators in eqs. (13) – (15), we define $\mathbf{f}_{(1,\beta_1,\alpha)} = \mathbf{g}_\alpha \circ \mathbf{h}_{\beta_1,1}$ and $\mathbf{f}_{(2,\beta_2,\alpha)} = \mathbf{g}_\alpha \circ \mathbf{h}_{2\beta_2,\frac{1}{2}}$. Then $\mathbf{F}_{(1,\beta,\alpha)} = \mathbf{f}_{(1,\beta,\alpha)}$, but $\mathbf{F}_{(2,\beta,\alpha)} = \mathbf{f}^2_{(2,\frac{\beta}{2},\alpha)}$.

Similar caricatures are formed for more general $\frac{m}{n}$ by interrupting the time one flow of eq. (16) with "kicks" of amplitude $\alpha_1 = \alpha(2-\gamma)$ every $\frac{1}{m}$ seconds, and of amplitude $\alpha_2 = \alpha(\gamma-1)$ every $\frac{1}{n}$ seconds. At time 1 we arbitrarily choose to kick with magnitude α_1 before the kick of magnitude α_2.

Remark: Note that $\mathbf{f}_{(1,\beta_1,\alpha)}$ and $\mathbf{f}_{(2,\beta_2,\alpha)}$ are not equal in our caricature, even though $\mathbf{W}_1 = \mathbf{W}_2$ in the theoretical setting of eq. (3) would imply $\mathbf{f}_{(1,\beta_1,\alpha)} = \mathbf{f}_{(2,\beta_2,\alpha)}$, using the definitions of eqs. (13) – (15). This disadvantage, however, is only aesthetic, and not significant in terms of our results. Given the choice between the aesthetics of a true model, and the ease of computation of the caricature, we have chosen the caricature's ease of computation.

4.2 Parameter plane bifurcation diagrams

Figure 3 shows (β, α) parameter plane bifurcation diagrams for eq. (17) for a sequence of auxiliary parameter γ values. As noted in the "Periodically forced oscillator maps" paragraph of Section 2, we expect the bifurcation diagrams to have distinctive shapes according to their period: triangular for period one, ice cream cone for period two, rounded top for period three, rounded or wedge top for period four, and cusped top for periods greater than five. This is the generic case, in the absence of any symmetry.

The 1/1 resonance region. It has the characteristic triangular shape of a period one resonance region at $\gamma = 1$, but develops a flame sometime before $\gamma = 1.7$. The size of the flame grows as γ increases. The number of fixed points in various subregions is indicated in the enlargement of Fig. 4. This shows the extra pair of fixed points that exist inside the flame. The fixed point that exists outside the triangle and outside the flame is the continuation from $\alpha = 0$ of the repelling fixed point at the origin. As γ increases beyond 1.9, the flame continues to grow and becomes part of the ice cream cone shape, characteristic of a period-two region, by $\gamma = 2$. The number of fixed points at $\gamma = 2$ corresponds to the number of period-2 points inside a simple period-two region plus one extra point for the continuation of the repelling fixed point. The top cusp becomes less and

less prominent, finally smoothing out at $\gamma = 2$. Note also that the period doubling circle PD_1 for $\mathbf{f}_{(2,\beta,\alpha)}$ is a pitchfork circle PF_1 for the second iterate, $\mathbf{F}_{(2,\beta,\alpha)}$. The symmetry of the pitchfork is broken as γ decreases from 2, leaving in its place the saddle-node bifurcation curve SN_1.

The 1/2 region. It has the ice cream cone shape of a period-two region at $\gamma = 1$. As γ increases from one, the period doubling circle, which is the ice cream part of the ice cream cone, shrinks. Simultaneously, a flame is born sometime between $\gamma = 1.7$ and $\gamma = 1.9$. See the enlargement in Fig. 4: an extra pair of period-2 orbits (four period-2 points) exists for parameter values inside the flame. The flame continues to grow inside the resonance region while the period doubling circle and the whole resonance region shrink. Finally, at $\gamma = 2$, the flame and the outside of the region have merged. In the process the circle has shrunk to the tip point at the top of the resonance region; the upper tip of the flame simultaneously arrives at this point as well. The shape at $\gamma = 2$ is characteristic of a period-four region.

The $\frac{3}{4}$ region. The region evolves from a period-four shape at $\gamma = 1$ to a period-eight shape at $\gamma = 2$. (The period-four and period-eight shapes are distinguishable only by the higher order contact at the upper (Hopf) tip. In general, the period-eight region is thinner than a period-four region.) Somewhere between $\gamma = 1.9$ and $\gamma = 2$ a flame appears inside the resonance region. This flame grows as γ increases, finally merging with the outside edge of the resonance region as γ reaches two. Simultaneously, the upper tip of the flame arrives at the upper tip of the region, and the lower tip of the flame arrives at the lower tip of the region. The number of period-4 orbits inside the region has gone from 2 at $\gamma = 1$ to 4 at $\gamma = 2$.

The $\frac{2}{1}$ and $\frac{2}{3}$ regions. No significant changes in the shape of the resonance regions, or in the number of orbits which exist, occur as γ varies between one and two. The former all are characteristic triangles, and the latter, although not very visible in the figure, remain characteristic of period-three regions — all with rounded tops.

Other $\frac{p}{q}$ regions. In general, a $\frac{p}{q}$ region changes from a $\frac{p}{q}$ shape into a $\frac{p}{2q}$ shape as γ increases from 1 to 2. If 2 divides p, no qualitative change need result: $\frac{p}{2q}$ and $\frac{p}{q}$ both correspond to period q. If 2 does not divide p, then the change is from a period-$2q$ region into a period-q region, and a flame will necessarily exist near $\gamma = 2$. This is consistent with the statements made at the end of Section 3.

4.3 Resonance surfaces

As with the singly forced oscillator studies, the parameter plane bifurcation diagrams can be much better understood when viewed as projections to the parameter plane of periodic point surfaces in the four-dimensional phase × parameter space. Because the actual resonance regions for the weak resonance case are so narrow, we choose to illustrate with a schematic diagram instead (but still for the $m = 1, n = 2$ case). A sequence of $\frac{1}{5}$ resonance surfaces with corresponding saddle-node curves is displayed in Fig. 5. The surfaces should also be compared to the "flame" from the circle map setting in Fig. 2. (The definitions of resonance surface and resonance region, as well as a description of the orbit identification which was used in displaying the sequence of surfaces, were given earlier in subsection 2.3.1.) At $\gamma = 1$ the simplest form of a $\frac{1}{5}$ resonance surface and region exist. As γ increases, an extra fold in the surface develops and grows; this projects to the flame in the region. The edges of the extra fold exactly line up with the edges of the "original" fold, both projecting to the region boundary at $\gamma = 2$. Since we have portrayed orbits rather than points in the $\frac{1}{5}$ surfaces of Fig. 5, the figure would be qualitatively identical for any $\frac{p}{q}$ surface with $q \geq 5$ and odd. Although the strong resonance surfaces, especially for $q = 1$ or 2, are quite different from the weak resonance surfaces, the flames in these special cases can still be viewed as projections of more natural folds in the corresponding resonance surfaces.

5 A True Doubly Periodically Forced Oscillator

Although we believe that the caricature on which we performed most of our numerical experiments is sufficient to illustrate our results, we provide corroboration in this section using a "true" doubly periodically forced oscillator.

Our example is the periodically forced Brusselator, a useful caricature of a homogeneous, autocatalytic kinetic scheme capable of self oscillations, which has repeatedly served as the main illustrative example for both the relevant phenomenology [KT 79] as well as various computer assisted approaches to periodically forced oscillator dynamics [KSA 1986, KAS 1986]. Periodic focing of chemical processes, as a means to obtain better average performance (selectivity, reactivity) compared to steady state operation is a subject with a long history, which is particularly interesting again today in the context of the so-called reverse-flow reactors (see Bailey [Ba 1973] for one of the first reviews of the subject).

The relevant single-frequency doubly-forced equations, exactly in the form of eq. (2), are

$$\begin{aligned} \dot{x} &= A + x^2 y - Bx - x + \alpha[(2-\gamma)\cos(2\pi\omega t) + (\gamma - 1)\cos(4\pi\omega t)] \quad (18) \\ \dot{y} &= Bx - x^2 y \end{aligned}$$

We choose the same "base case" of $A = 0.4, B = 1.2$ as in earlier singly forced

studies [KT 1979, AMKA 1986]. For these parameter values, the autonomous ($\alpha = 0$) oscillator frequency is $\omega_0 = 0.3750375$. By making the same parameter change as suggested in the introduction, $\beta = \omega_0/\omega$, and computed the 1/1 resonance region for several fixed values of the relative forcing amplitude parameter, γ. We show in Fig. 6 the result for $\gamma = 1.7$. This figure should be compared to the caricature results for the 1/1 region of Fig. 3 for the $\gamma = 1.9$ case. The flame which was guaranteed to exist at $\gamma = 2$ is still present at $\gamma = 1.7$. There are some differences between the two figures which are worth pointing out. The flame in the Brusselator example extends to the zero forcing amplitude tip of the resonance region, but doesn't in the caricature. (See Remark 2 at the end of Section 6.1.) Also the cusp at the top of the flame in the caricature is instead on the triangular saddle-node curve (here triangular plus the extra cusp). From numerical continuations not presented here, we know that as γ is further decreased from 1.7, the size of the flame will decrease, and the flame and triangular region will interact, leaving by $\gamma = 1$ a triangular region with no extra cusp, and no flame.

6 Local symmetry breaking analysis

The majority of this paper has dealt with explaining what happens to resonance surfaces and corresponding bifurcation diagrams as our auxiliary parameter γ is varied. In this section, we use a combination of local analysis and Fourier series to analyze the local symmetry breaking at the two resonance region tips. More specifically, we have already explained in Section 3 why $\mathbf{F}_{(2,\beta,\alpha)}$ being the n^{th} iterate of $\mathbf{f}_{(2,\frac{\beta}{n},\alpha)}$ causes extra orbits to exist throughout a $\frac{p}{q}$ resonance region at $\gamma = 2$ whenever $\gcd(n, q_2) > 1$. We now describe what happens near the two tips asa γ is perturbed from two.

Proposition 6.1 *The following behavior is generic for the (β, α) parameter plane bifurcation diagram for the stroboscopic families, $\mathbf{F}_{(\gamma,\beta,\alpha)}$, defined in eq. (13) via the doubly forced oscillator in the form of eq. (3):*

1. *Flames persist in the $\alpha = 0$ tip of any $\frac{p}{q}$ resonance region with $q_2 = q \cdot \gcd(n, q_2)$ as γ is decreased from 2 whenever $\gcd(n, q_2) > 1$. That is, given any $\frac{p}{q}$, there exist $\delta_\gamma > 0$ and $\delta_\alpha > 0$ such that for $\gamma \in [2, 2 - \delta_\gamma)$ the subregion of the $\frac{p}{q}$ resonance region in the (β, α) parameter plane for which the corresponding maps have more than two period-q orbits intersects the $\alpha = \alpha_0$ line for any $\alpha_0 \in (0, \delta_\alpha)$.*

2. *Flames do not persist in the Hopf tip of any $\frac{p}{q}$ resonance region with $q_2 = q \cdot \gcd(n, q_2) > q \geq 5$ as γ is decreased from 2. That is, given any $\frac{p}{q}$, and any γ sufficiently close to, but not equal to 2, the subregion of the $\frac{p}{q}$ resonance*

region in the (β, α) parameter plane for which the corresponding maps have more than two period-q orbits (restricting, if necessary to a neighborhood of the p/q resonant Hopf point in the phase space) does not extend to the p/q Hopf point at the tip of the p/q resonance region.

Analogous results hold for γ near 1.

Similar statements are true for the strong resonance cases ($q < 5$), but the justification requires a division into may cases, each of which is substantial to analyze. But in general, if $q_2 = kq$, there are $k - 1$ flames in the $\frac{p}{q}$ resonance region for $\mathbf{F}_{(\gamma,\beta,\alpha)}$ for γ sufficiently close to 2.

The first claim is justified using Fourier series analysis since the forced oscillator maps can be reduced to circle maps for small forcing amplitude. The second claim is justified using local normal forms analysis in the neighborhood (of phase $\times$ parameter space) of a $\frac{p}{q}$ Hopf point. We will assume for convenience that the original differential equation (eq.(3)) is C^∞ in all of its variables and parameters. This implies that the corresponding stroboscopic maps $\mathbf{F}_{(\gamma,\beta,\alpha)}$ and $\mathbf{f}_{(2,\beta,\alpha)}$ are also C^∞.

6.1 Small forcing analysis. (Proof of Proposition 6.1, Part 1.)

As in the singly forced oscillator setting described in Section 2, the original unforced oscillator limit cycle C in the doubly forced oscillator setting persists as an invariant circle for the stroboscopic maps $\mathbf{F}_{(\gamma,\beta,\alpha)}$ as the forcing amplitude α is increased from zero. We label this perturbed invariant circle $C_{(\gamma,\beta,\alpha)}$. It is guaranteed to exist for α sufficiently small. Analgous to our notation in subsection 2.2, we denote the lift of the circle maps obtained by restricting $\mathbf{F}_{(\gamma,\beta,\alpha)}$ to $C_{(\gamma,\beta,\alpha)}$ by $\tilde{F}_{(\gamma,\beta,\alpha)}$. As noted in subsection 2.2, because the maps at $\alpha = 0$ are all conjugate to a rigid rotation with rotation number β, and by calling the conjugate map by the same name, we can assume that $\tilde{F}_{(\gamma,\beta,\alpha)}$ has the following form:

$$\tilde{F}_{(\gamma,\beta,\alpha)} : u \mapsto u + 2\pi\beta + \alpha G_{(\gamma,\beta,\alpha)}(u) \tag{19}$$

where $u \in \mathcal{R}^1$, and G is periodic with period 2π. Note that $G_{(\gamma,\beta,\alpha)}(u)$ is defined by $\dfrac{\partial \tilde{F}_{(\gamma,\beta,\alpha)}(u)}{\partial \alpha}$.

A $\frac{p}{q}$ point ($\frac{p}{q}$ reduced) is defined by

$$\tilde{F}^q_{(\gamma,\beta,\alpha)}(u) = u + 2\pi p \tag{20}$$

A $\frac{p}{q}$ point will be a period-q point with rotation number $\frac{p}{q}$ for the associated circle map.

Lemma 6.2 *For $k \geq 1$, $\tilde{F}^k_{(\gamma,\beta,\alpha)}(u) = u + k2\pi\beta + \alpha \sum_{j=0}^{k-1} G_{(\gamma,\beta,\alpha)}(\tilde{F}^j_{(\gamma,\beta,\alpha)}(u))$.*

PROOF Straightforward computation using eq. (19) and induction. ◇

Lemma 6.2 allows us to rewrite the condition for a $\frac{p}{q}$-point in eq. (20) as a zero of $H(\gamma, \beta, \alpha, u)$, where

$$H(\gamma,\beta,\alpha,u) = \tilde{F}^q_{(\gamma,\beta,\alpha)}(u) - u - 2\pi p = 2\pi q(\beta - \frac{p}{q}) + \alpha \sum_{j=0}^{q-1} G_{(\gamma,\beta,\alpha)}(\tilde{F}^j_{(\gamma,\beta,\alpha)}(u)) \quad (21)$$

We note that $H(\gamma, \frac{p}{q}, 0, u) = 0$ for all γ and u, and $\dfrac{\partial H}{\partial \beta}(\gamma, \beta, 0, u) = 2\pi q$ for all γ, β and u. So we can use the implicit function theorem to solve $H(\gamma, \frac{p}{q}, 0, u) = 0$ for β near $\alpha = 0$ to obtain:

$$\begin{aligned}
\beta(\gamma,\alpha,u) &= \beta(\gamma,0,u) + \alpha\frac{\partial\beta}{\partial\alpha}(\gamma,0,u) + O(\alpha^2) \\
&= \frac{p}{q} - \frac{\alpha}{2\pi q}(\frac{\partial H}{\partial\alpha}(\gamma,\frac{p}{q},0,u) + O(\alpha)) \\
&= \frac{p}{q} - \frac{\alpha}{2\pi q}(\frac{\partial H}{\partial\alpha}(2,\frac{p}{q},0,u) + O(\gamma-2,\alpha)) \qquad (22)
\end{aligned}$$

To complete the proof, our task is to show that, for γ fixed sufficiently close to 2, and α fixed sufficiently close to 0 (but not equal to zero), $\beta(\gamma, \alpha, u)$ takes on some value more than $2q$ times for $u \in [0, 2\pi)$. We do this by showing that $\frac{\partial H}{\partial\alpha}(2, \frac{p}{q}, 0, u)$ (generically) has this "$2q$ value" property, and then, by the form of eq. (22) and continuity in γ and α, the property also holds for $\beta(\gamma, \alpha, u)$ for γ and α sufficiently close to 0 and 2, respectively. The heueristic reason that $\frac{\partial H}{\partial\alpha}(2, \frac{p}{q}, 0, u)$ has the property is because of the symmetry at $\gamma = 2$: its values, being associated with orbits of period-q_2, where $q_2 = q \cdot \gcd(n, q_2)$, come in groups of q_2. Since the orbits themselves come in pairs (an attracting and a repelling), there will be values of $\frac{\partial H}{\partial\alpha}(2, \frac{p}{q}, 0, u)$ that are taken on $2q_2$ times. The formal computation of $\frac{\partial H}{\partial\alpha}(2, \frac{p}{q}, 0, u)$ follows.

By the same assumptions we used to obtain the form of $\tilde{F}_{(\gamma,\beta,\alpha)}$ in eq. (19) we can assume the form of $\tilde{f}_{(2,\beta,\alpha)}$, the lift of $\mathbf{f}_{(2,\beta,\alpha)}$ restricted to the corresponding invariant circle, to be

$$\tilde{f}_{(\gamma,\beta_2,\alpha)} : u \mapsto u + 2\pi\beta_2 + \alpha g_{(2,\beta_2,\alpha)}(u) \quad (23)$$

where $g_{(2,\beta_2,\alpha)}$ is some period-2π function. Recalling that $\beta_2 = \frac{\beta}{n}$ and that $\mathbf{F}_{(2,\beta,\alpha)} = \mathbf{f}^n_{(2,\frac{\beta}{n},\alpha)}$, Lemma 6.2 now implies

$$H(2,\beta,\alpha,u) = \tilde{f}^{nq}_{(2,\frac{\beta}{n},\alpha)}(u) - u - 2\pi p = 2\pi nq(\frac{\beta - \frac{p}{q}}{n}) + \alpha \sum_{j=0}^{nq-1} g_{(2,\frac{\beta}{n},\alpha)}(\tilde{f}^j_{(2,\frac{\beta}{n},\alpha)}(u)).$$

Since $g_{(2,\beta_2,\alpha)}(u)$ is period 2π in u, it can be expressed in a Fourier series as

$$g_{(2,\beta_2,\alpha)}(u) = \sum_{l=-\infty}^{\infty} c_l(2,\beta_2,\alpha)e^{ilu}.$$

So we can compute

$$\begin{aligned}
\frac{\partial H}{\partial \alpha}(2,\frac{p}{q},0,u) &= \sum_{j=0}^{nq-1} g_{(2,\frac{p}{nq},0)}(\tilde{f}^j_{(2,\frac{p}{nq},0)}(u)) \\
&= \sum_{j=0}^{nq-1}\sum_{l=-\infty}^{\infty} c_l(2,\frac{p}{nq},0)e^{il(u+2\pi j\frac{p}{nq})} \\
&= \sum_{j=0}^{nq-1}\sum_{l=-\infty}^{\infty} c_l(2,\frac{p}{nq},0)e^{il(u+2\pi j\frac{p_2}{q_2})}, \text{ since} \frac{p}{nq} = \frac{p_2}{q_2} \\
&= \sum_{l=-\infty}^{\infty} c_{lq_2}(2,\frac{p_2}{q_2},0)nqe^{ilq_2u}. \qquad (24)
\end{aligned}$$

The last equality is obtained by switching the order of summation and noting that $\sum_{j=0}^{nq-1} e^{il2\pi j\frac{p_2}{q_2}}$ is nq for l a multiple of q_2 and 0 otherwise. This last form for $\frac{\partial H}{\partial \alpha}(2,\frac{p}{q},0,u)$ also shows that, being invariant to translations in u by multiples of $\frac{2\pi}{q_2}$, $\frac{\partial H}{\partial \alpha}(2,\frac{p}{q},0,u)$ takes on the same value for q_2 values of u at a time. Furthermore, by continuity, for any values it takes on strictly between its global maximum and minimum (each of which must also be taken on at least q_2 times), it must take on the same value for $2q_2$ values of u at a time. (Think of $\sin(q_2u)$, which takes on every value in the interval $(1,-1)$ $2q_2$ times for $u \in [0,2\pi)$, but takes on its maximum and minumum only q_2 times.) Our generic condition that must be satisfied to have a value strictly between the global maximum and minimum of $\frac{\partial H}{\partial \alpha}(2,\frac{p}{q},0,u_0)$ is that $\frac{\partial H}{\partial \alpha}(2,\frac{p}{q},0,u_0)$ not be constant. That is, at least one coefficient $c_{lq_2}(2,\frac{p_2}{q_2},0)$ with $l \neq 0$ must be nonzero. This completes the proof.

Remarks.

1. **The separation condition.** The proposition just proved shows that we expect flames to persist in the $\alpha = 0$ tip of a resonance region as γ is perturbed from 2. On the other hand, the flame could separate from the $\alpha = 0$ tip for α values "farther" away from 2. Our computations in the above proof give us a condition which must be satisfied at a specific value of γ where the separation takes place. In the simplest case, the function $\frac{\partial H}{\partial \alpha}(\gamma,\frac{p}{q},0,u)$ needs to go from having q_2 maximum points and q_2 minimum points at $\gamma = 2$ to having q of each. The only way for a smooth periodic function to lose local extrema is to pass through a value (of γ) for which

there is an extremum which is also an inflection point. So the condition (necessary, but not sufficient) for a flame to separate at $\gamma = \gamma_s$ is to have a point u_s for which $S'(u_s) = 0$ and $S''(u_s) = 0$, where $S(u) = \frac{\partial H}{\partial \alpha}(\gamma_s, \frac{p}{q}, 0, u)$. Of course certain nondegeneracy conditions must also be satisfied, and when there are multiple flames, each flame must go through such a condition to separate, but we do not deal with these details here.

2. **Nongenericity of our doubly forced oscillator caricature.** We note that, while Proposition 6.1 holds (as far as we can tell) for the Brusselator example, part 1 of our Proposition does not hold for our doubly forced oscillator caricature. So our caricature example is actually nongeneric. None of the flames pictured in Fig. 3 for any $\gamma < 2$ extend into the zero forcing amplitude tip of the corresponding resonance region. On the other hand, the flame for the Brusselator example in Fig. 6 still extends into the zero forcing amplitude region of the 1/1 resonance region when γ has been decreased all the way from 2 to 1.7.

   We argue, however, that the caricature (eq. (17)) we used in this paper as our primary numerical example, is still representative of the behavior of typical physical system models, even though it is nongeneric in this one specific feature. Furthermore, the nongenericity (having an infinity of vanishing Fourier series coefficients) is certainly quite typical of examples of periodically forced oscillators that arise as models of physical systems. The standard circle map family, for example, with forcing function $g(u) = \sin(u)$, has only one nonzero coefficient in its expansion. Similarly, in our caricature, the map $\tilde{f}_{(2,\beta_2,0)}$ ($\mathbf{f}_{(2,\beta_2,0)}$ restricted to the invariant circle) is the standard map to first order terms in α [Mc 1992]. In this "standard map case," all the coefficients $c_{lq_2}(2, \frac{p_2}{q_2}, 0)$ in eq. (24) vanish whenever $q_2 > 1$, so all the terms are $O(\alpha(\gamma - 2) + \alpha^2)$. At $\gamma = 2$, all terms must be $O(\alpha^2)$. (This implies that the associated Arnold tongue has sides that are tangent at $\alpha = 0$; that is, the tongues are cusps, not the generic wedges that open at a finite angle.) After perturbing γ from 2, however, terms of order $\alpha O(\gamma - 2)$ could dominate the terms which are $O(\alpha^2)$. That is, the small α behavior at $\gamma = 2$ does not necessarily persist when γ is decreased from 2. Thus the flames in our caricature are allowed to (and numerically do) separate from the $\alpha = 0$ tip of the respective $\frac{p}{q}$ resonance region as soon as γ has any value less than 2. For related examples using Fourier series analysis, see Hall [Ha 1984], McGehee and Peckham [MP 1996], and Broer, Simó and Tatjer [BST 1998].

6.2 Hopf bifurcation analysis (Proof of Proposition 6.1, Part 2.)

In this section we provide a brief explanation of how the symmetry breaking causes the flame(s) which extends to the (upper) Hopf tip of the $\frac{p}{q}$ resonance region for $\mathbf{F}_{(2,\beta,\alpha)}$ to separate from the Hopf tip of the $\frac{p}{q}$ resonance region for $\mathbf{F}_{(\gamma,\beta,\alpha)}$ when γ is decreased from 2. Recall that we are considering γ as an auxiliary parameter, so the resonance regions all live in the (β, α) parameter plane for fixed values of γ. The "no flame" explanation is essentially a direct result of the analysis of a resonant Hopf bifurcation point [Ar 1977, Ar 1983, Ta 1974] where it is shown that generically (avoiding the low order resonance cases with $q \leq 4$), for parameter values interior to the p/q resonance region, and sufficiently close to its Hopf tip, the corresponding maps have exactly two period-q orbits: one saddle and one node. Our maps fail to satisfy the generic condition at $\gamma = 2$, but are assumed to satisfy the condition for γ near 2. Since flames require the existence of "extra" period-q orbits, we have the following scenario. When $\gamma = 2$, there are $n - 1$ flames; they are, however, not visible in the paramter plane bifurcation diagram because the symmetry that guarantees their existence ($\mathbf{F}_{(2,\beta,\alpha)}$ is the n^{th} iterate of $\mathbf{f}_{(2,\frac{\beta}{n},\alpha)}$) also gurantees that saddle-node sides of the flames will all project to the the saddle-node sides of the resonance region (as in the $\mathbf{F}_{(2,\beta,\alpha)}$ part of Fig. 5). As γ is perturbed from two, since the flames can no longer (generically) extend to the Hopf tip, the $n - 1$ flame tips must pull away from the Hopf tip and into the interior of the resonance region. At this point they are visible in a parameter plane bifurcation diagram (as in the $\mathbf{F}_{(2-,\beta,\alpha)}$ part of Fig. 5).

A sketch of the argument follows below. We note that in the references of the previous paragraph, the authors work directly with equivariant vector fields. The connection to the map case is drawn by showing that the q^{th} iterate of the maps are, up to arbitrarily high order, conjugate to time-one maps of these equivariant vector fields. We choose a more direct approach, working with the maps themselves. The calculations are quite similar to arguments presented elsewhere [PFK 1995]. That paper contains more details than we include here. It was a study of a degeneracy in a $\frac{p}{q}$ resonant Hopf bifurcation, but included as well computations for the nondegenerate case. It is the nondegenerate case we use in this paper. A singularity theory approach such as in Peckham and Kevrekidis [PK 1991] or more specifically for the Hopf bifurcation as in Broer and Golubitsky [BG 2002] could also have been used here.

Sketch of proof. Rewrite $\mathbf{F}_{(\gamma,\beta,\alpha)}$ in normal form by perfoming the following changes of variables. Translate the unique local fixed point to the origin. Change the phase variable to complex "$(\mathbf{z}, \overline{\mathbf{z}})$" coordinates (where $\overline{\mathbf{z}}$ is the complex conjugate of $\mathbf{z}$): $\mathbf{x} = (x_1, x_2) \rightarrow x_1 + ix_2 = \mathbf{z}$. Eliminate all "low order" nonresonant terms. The linear term cannot be eliminated. Other resonant terms which cannot

be eliminated are divided into two groups: those that are independent of the angle of $\mathbf{z}$ after factoring out $\mathbf{z}$ (the $\mathbf{z}^j\overline{\mathbf{z}}^{j-1}$ terms for $j = 2, 3, \cdots$) and those that aren't. It turns out that it is important to keep the lowest order terms in each group. The lowest "theta independent" term is the $\mathbf{z}^2\overline{\mathbf{z}}$ term. The lowest order "theta dependent" term is the $\overline{\mathbf{z}}^{q-1}$ term when $\gamma < 2$, but it is the $\overline{\mathbf{z}}^{q_2-1}$ term when $\gamma = 2$. (Recall that $\mathbf{F}_{(2,\beta,\alpha)}$ is the n^{th} iterate of $\mathbf{f}_{(2,\frac{\beta}{n},\alpha)}$. This means that the lowest order theta dependent term for $\mathbf{f}_{(2,\frac{\beta}{n},\alpha)}$ is the $\overline{\mathbf{z}}^{q_2-1}$ term. It is a (straightforward, but nontrivial) computation that the lowest order theta dependent term for $\mathbf{F}_{(2,\beta,\alpha)}$ is also the $\overline{\mathbf{z}}^{q_2-1}$ term.)

Next, we change parameters from (γ, β, α) to (γ, ρ, ϕ) where $\rho(\gamma, \beta, \alpha)$ and $\phi(\gamma, \beta, \alpha)$ are defined by requiring the eigenvalue of the (unique) fixed point for $\mathbf{F}_{(\gamma,\beta,\alpha)}$ to be $e^{2\pi i p/q}\rho e^{i\phi}$. Note that this makes the point $(\rho, \phi) = (0, 0)$ the Hopf tip of the p/q resonance region in the "new" parameter plane for each fixed γ near 2. Our first generic assumption is that this parameter change is nonsingular at $(\gamma, \rho, \phi) = (2, 0, 0)$.

Thus, we can assume the map $\mathbf{F}_{(\gamma,\beta,\alpha)}$ has the following (normal) form:

$$\begin{aligned}\mathbf{F}_{(\gamma,\rho,\phi)}(z) &= e^{2\pi i\frac{p}{q}}e^{\rho(\gamma)+i\phi(\gamma)}(\mathbf{z} + A_\gamma(\rho,\phi)\mathbf{z}^2\overline{\mathbf{z}} + \cdots \\ &\quad + (\gamma-2)\widetilde{B}_\gamma(\rho,\phi)\overline{\mathbf{z}}^{q-1} + \cdots + B_\gamma(\rho,\phi)\overline{\mathbf{z}}^{q_2-1} + \cdots).\end{aligned}$$

We have factored out the eigenvalue of the fixed point for computational convenience in the steps that follow. We have also taken out the factor of $(\gamma - 2)$ from the $\overline{\mathbf{z}}^{q-1}$ term since the symmetry makes it a nonresonant term, and thus zero in normal form, at $\gamma = 2$. Our critical generic assumption is that the coefficient $\widetilde{B}_2(0, 0)$ is nonzero.

At this point, we need only solve $\mathbf{F}^q_{(\gamma,\rho,\phi)}(\mathbf{z}) - \mathbf{z} = \mathbf{0}$ for period-q points and interpret the results. There are two cases: $\gamma = 2$ for which we can ignore the $\overline{\mathbf{z}}^{q-1}$ term, and $\gamma < 2$, for which we can ignore the $\overline{\mathbf{z}}^{q_2-1}$ term. Each case separately comes out of the "standard" analysis of the nondegenerate resonant Hopf bifurcation referred to above. By computing $\mathbf{F}^q_{(\gamma,\rho,\phi)}(\mathbf{z})-\mathbf{z}$, changing to polar coordinates via $z = re^{i\theta}$, dividing by r to eliminate the fixed-point solutions, expanding in terms of the small parameters ρ and ϕ and powers of $\gamma - 2$, we use the implicit function theorem to obtain the least-period-q points as

$$\rho+i\phi = -A_2(0,0)r^2 - \cdots - (\gamma-2)\widetilde{B}_2(0,0)r^{q-2}e^{-qi\theta} - \cdots - B_2(0,0)r^{q_2-2}e^{-q_2 i\theta} - \cdots.$$

All omitted terms are dominated by terms written above, in powers of r and $\gamma-2$. We assume that the coefficients That all three coefficients $A_2(0, 0)$ and $B_2(0, 0)$ are nonzero. These two nonzero coefficients, along with the above-mentioned assumptions that $\widetilde{B}_2(0, 0)$ is nonzero and that the parameter change from (γ, β, α) to (γ, ρ, ϕ) is nonsingular are our generic assumptions.

We now interpret the least-period-q solution. For any $\gamma < 2$ we see that the term $(\gamma - 2)\widetilde{B}_\gamma(0, 0)r^{q-2}e^{-qi\theta}$ dominates the term $B_\gamma(0, 0)r^{q_2-2}e^{-q_2 i\theta}$ for r

sufficiently small. Since we are restricting ourselves to the weak resonance cases, the Ar^2 term dominates all other terms. It can then be seen that (neglecting higher order terms) the projection to the (ρ, ϕ) parameter plane of the period-q solution set of $\rho + i\phi = -A_\gamma(0,0)r^2 - ((\gamma-2)\widetilde{B}_\gamma(0,0)r^{q-2}e^{-qi\theta}$ covers a cusp-shaped resonance region. By fixing r sufficiently small and varying θ from 0 to 2π, a circle in this resonance region is swept out and covered q times. Since each time around the circle corresponds to once back and forth across the resonance region, and each passage across the resonance region corresponds to a different $\frac{p}{q}$ point, there are $2q$ distinct period-q points, corresponding to 2 orbits, for each (ρ, ϕ) in the interior of the resonance region and near the cusp. A similar argument gives $2q_2 = 2nq > 2q$ solutions if $\gamma = 2$. Therefore, generically, flames extend to the Hopf tip of a p/q resonance region at $\gamma = 2$, but no flames persist all the way to the Hopf point for $1 << \gamma < 2$. This completes the sketch of the proof.

7 Acknowledgements

The authors acknowledge many conversations over the years with D. G. Aronson, G. R. Hall, R. P. McGehee and R. Moeckel whch have helped develop many of the ideas presented in this paper. Support of both authors by the the National Science Foundation is also gratefully acknowledged.

References

[Ar 1965] Arnold V.I., "Small Denominators. I. Mappings of the circumference onto itself," *AMS Translations*, Series 2, **46**, 213-284, 1965.

[Ar 1977] Arnold V.I., "Loss of stability of self oscillations close to resonances and versal deformations of equivariant vector fields," *Func. Anal. Appl.*, **11** (2), 1–10, 1977.

[Ar 1983] Arnold V.I., *Geometrical Methods in the Theory of Ordinary Differential Equations*, Springer-Verlag, New York, 1983.

[AMKA 1986] Aronson D.G., McGehee R.P., Kevrekidis I.G., Aris R., "Entrainment Regions for Periodically Forced Oscillators," *Phys. Rev. E* **33** (3) 2190-2192, 1986.

[Ba 1987] Baesens C., "Systemes dynamique dissipatifs forces periodiquement: orbites homocline, bifurcations blobales et chaos," Dissertation, Université Libre de Bruxelles, 1987.

[BGKM 1991a] Baesens C., Guckenheimer J., Kim S., McKay R.S., "Simple Resonance Regions of Torus Diffeomorphisms," *Patterns and Dynamics of Reactive Media* (Aris R, Aronson D G & Swinney H L eds.), IMA Volumes in Mathematics and its Applications, 37, 1–11, 1991.

[BGKM 1991b] Baesens C., Guckenheimer J., Kim S., McKay R.S., "Three Coupled Oscillators: Mode-locking, Global Bifurcations and Toroidal Chaos," *Physica D*, 49, 387–485, 1991.

[Ba 1973] Bailey J.E., "Periodic Operation of Chemical Reactors: A review," *Chem. Eng. Commun.* **1** 111-124, 1973.

[Bo 1976] Bogdanov R.I.,"Versal deformation of a singularity of a vector field in the plane in the case of zero eigenvalues," *Trudy Seminara Imeni I. G. Petrovskogo* **2**, 23-36, 1976. English translation: *Selecta Math. Sovietica* **1**, No. 4, 389-421, 1981.

[BG 2002] Broer H W and Golubitsky M, "The Geometry of Resonance Tongues: A Singularity Theory Approach," preprint.

[BST 1998] Broer H, Simó C and Tatjer J, "Towards global models near homoclinic tangencies of dissipative diffeomorphisms," *Nonlinearity* **(11)** 667-770, 1998.

[Do 1981] Doedel E.J., "AUTO: a program for the automatic bifurcation analysis of autonomous systems", *Cong. Num.* **30**, 265-284, 1981.

[DK 1986] Doedel E.J. and Kernévez J.P., "AUTO: Software for continuation and bifurcation problems in ordinary differential equations (including the AUTO User Manual)," Report, Applied Mathematics, California Institute of Technology, 1986, 1994. The software and associated documentation is available via anonymous ftp at ftp.cs.concordia.ca.

[Ga 1985] Gambaudo J.M., "Perturbation of a Hopf Bifurcation by an External Time-Periodic Forcing," *J. Diff. Equ.* **57**, 172-199, 1985.

[GFPS 2000] Glendinning P, Feudel U, Pikovsky A S, and Stark J, " Structure of mode-locked regions in quasi-periodically forced circle maps," *Phyisca D* **140**, Issue 1–2, 227-243, 2000.

[Ha 1984] Hall G.R., "Resonance Zones in two-parameter families of circle homeomorphisms," *SIAM J. Math. Anal.***15** (6), 1075-1081, 1984.

[KT 1979] Kai T., Tomita K., "Stroboscopic phase portrait of a forced nonlinear oscillator," *Progr. Theor. Phys.*, **61**(1), 54-73, 1979.

[KAS 1986] Kevrekidis I.G., Aris R., Schmidt L.D., "The Stirred Tank Forced," *Chem. Engng Sci.*, **41**(6), 1549-1560, 1986.

[KSA 1986] Kevrekidis I.G., Schmidt L.D., Aris R., "Some Common Features of Periodically Forced Reacting Systems," *Chem. Engng Sci.*, **41**(5), 1263-1276, 1986.

[LK 1988] Leis, J.R. and Kramer, M.A., ODESSA an ordinary differential equation solver with explicit simultaneous sensitivity analysis, *ACM Trans Math Software* **14**, 61-67, 1988.

[Mc 1992] McGehee R.P., Unpublished computation, 1992.

[MP 1994] McGehee R.P. and Peckham B.B., "Resonance Surfaces for Forced Oscillators," Geometry Center Research Report GCG70 and *Experimental Mathematics* **3**, No. 3, 221-244, 1994.

[MP 1995] McGehee R.P. and Peckham B.B., "Determining the Global Topology of Resonance Surfaces for Periodically Forced Oscillator Families," *Normal Forms and Homoclinic Chaos*, Fields Institute Communications **4**, AMS, 233-251, 1995.

[MP 1996] McGehee R.P. and Peckham B.B., "Arnold flames and resonance surface folds," Geometry Center Research Report GCG84 and *International Journal of Bifurcations and Chaos* **6**, No. 2 (1996) 315-336.

[P 1990] Peckham, B.B.,"The Necessity of the Hopf Bifurcation for Periodically Forced oscillators with closed resonance regions," *Nonlinearity* **(3)** 261-280, 1990.

[P 2000] Peckham B.B., "Global parametrization and computation of resonance surfaces for periodically forced oscillators," *Numerical Methods for Bifurcation Problems and Large-Scale Dynamical Systems* (E. Doedel and L. Tuckerman, eds.), IMA Volumes in Mathematics and its Applications **119**, (New York: Springer), 385-405, 2000.

[P 1988-2001] Peckham B.B., *To Be Continued ...*, a continuation software package for discrete dynamical systems (continually under development), 1988-2001.

[PK 1991] Peckham B.B. and Kevrekidis I.G., "Period doubling with higher order degeneracies" *SIAM J. Math. Anal.* **22**, No. 6, 1552-1574, 1991.

[PFK 1995] Peckham B.B., Frouzakis C., and Kevrekidis I.G., "Bananas and Banana Splits: A parametric degeneracy in the Hopf bifurcation for maps," *SIAM J. Math. Anal.* **26**, No. 1, 190-217, 1995.

[Ph 1993] Phillips M, Levy S, Munzer T, "Geomview: An Interactive Geometry Viewer," *Notices of the Amer. Math. Soc.* **22**, 985-988, 1993.
This software and acompanying documentation are available at http://www.geom.umn.edu/software/download/geomview.html.

[SDCM 1988] Schreiber I., Dolnik M., Choc P., Marek M., "Resonance Behaviour in Two-Parameter Families of Periodically Forced Oscillators," *Physics Letters A*,**128, 2**, 66-70, 1988.

[Ta 1974] Takens F., "Forced oscillations and bifurcations," *Applications of Global Analysis* Communications of the Mathematical Institute Rijksuniversiteit Utrecht **3**, 1-59, 1974.

[Tay 1990] Taylor M.A., "Interactive AUTO: A Graphical Interface for AUTO86," Princeton University technical report, 1990.

[VR 1989] Vance W. and Ross J., "A detailed study of a forced chemical oscillator: Arnold Tongues and bifurcation sets," *J. Chem. Phys.*, **91** 7654-7670, 1989.

8 Figure Captions

1. Resonance surfaces for the Standard Family: $\theta \mapsto \theta + 2\pi\beta + \alpha\sin(\theta)$. See eq. (10) for the definition of the resonance surfaces which live in the cartesian product of the phase (variable θ) and parameter (variables β and α) spaces. The projection to the (β, α) parameter plane gives the familiar "Arnold tongue" picture. Figure reproduced from McGehee and Peckham [MP 1996].

2. An "Arnold flame" in a fixed-point resonace region for the map $\theta \mapsto \theta + 2\pi\beta + \alpha((0.1 + 0.9h(\alpha^2))\sin(\theta) + (0.9 - 0.9h(\alpha^2))\frac{\sin(2\theta)}{2}$ where $h(x)$ is a C^∞ function which increases from zero to one as x increases from zero to one. Compare with the flame for $\mathbf{F}_{(2-,\beta,\alpha)}$ in Fig. 5. Figure reproduced from McGehee and Peckham [MP 1996].

3. Resonance region melt in the (β, α) parameter plane as a function of the relative forcing parameter γ. The (β, α) bifurcation diagram for the stroboscopic maps $\mathbf{F}_{(\gamma,\beta,\alpha)}$ ($m = 1, n = 2$ in eq. (3)) evolves from the bifurcation diagram for $\mathbf{f}_{(1,\beta_1,\alpha)}$ (without rescaling since $m = 1$) to the bifurcation diagram for $\mathbf{f}_{(2,\beta_2,\alpha)}$ (with the rescaling $\beta = 2\beta_2$) as γ increases from 1 to 2. Flames are guaranteed to exist in every p/q resonance region with p odd and γ sufficiently close to 2, and are expected to disappear for γ sufficiently close to 1. Flames are visible here in the 1/1 region for $\gamma = 1.9$ and 1.7, and in the 1/2 region for $\gamma = 1.9$. Abbreviations for bifurcation curves: SN: saddle-node, PD: period doubling, H: Hopf. Subscripts denote the primary period of the bifurcating orbit.

4. Enlargement of the flames in the 1/1 and 1/2 resonance regions for $\mathbf{F}_{(1.9,\beta,\alpha)}$ in Fig. 3. The numbers indicate the number of *orbits* present for maps corresponding to parameters in each region (period-two orbits on the left, fixed points on the right). An extra pair of orbits exists for parameter values inside the flames. Abbreviations for bifurcation curves: SN: saddle-node, PD: period doubling, H: Hopf. For codimension-two bifurcation points: TB: Takens-Bogdanov (double +1 eigenvalues), DNO: Double Negative One eigenvalues, DPD: Degenerate Period Doubling (with one higher order degeneracy), C: cusp. Subscripts denote the primary period of the bifurcating orbit.

5. Schematic $\frac{1}{5}$ resonance surface melt as a function of the relative forcing parameter γ for the stroboscopic maps of eq. (13). Projection to the (x_1, β, α) space from the four-dimensional phase $\times$ parameter space. Further projection to the parameter plane is shown on the back face of the bounding boxes. The colors of the saddle-node curves on the surfaces corresond to the colors of their projections to the parameter plane. Insets show more clearly the projection to the parameter plane of the two flames. The resonance surface

evolves from the "singly folded" surface at $\gamma = 1$ to the "doubly folded" surface at $\gamma = 2$. Flames are guaranteed to exist for γ sufficiently close to 2, and are expected to disappear for γ sufficiently close to 1. See Section 2.3.1 for surface definitions, and Section 4.3 for further description.

6. Flame in the 1/1 resonance region in the (β, α) parameter plane for the stroboscopic map of the doubly forced Brusselator of eq. (19). The relative forcing parameter γ is 1.7. This figure should be compared to the 1/1 resonance region for the doubly forced caricature map, $F_{(1.9,\beta,\alpha)}$, in Figure 1. As in Figure 1, both curves are fixed-point saddle-node curves. As γ continues to decrease, the size of the flame will also decrease, disappearing entirely before $\gamma = 1$.

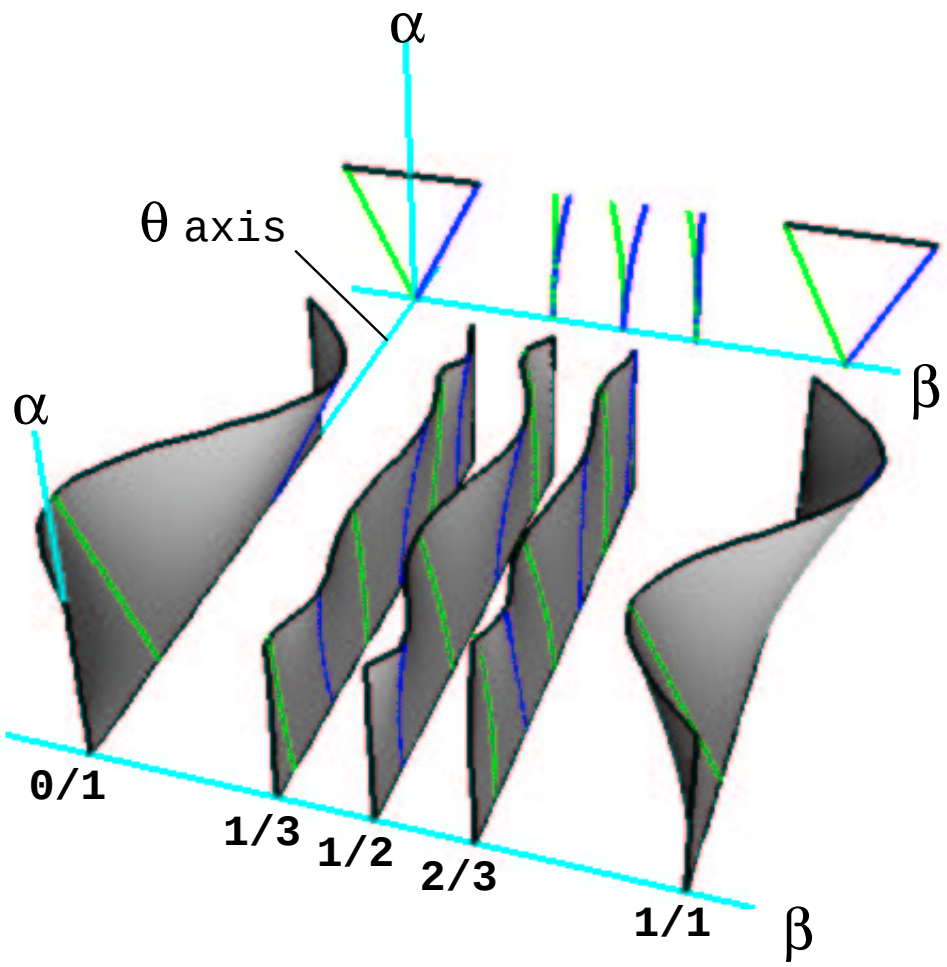

Figure 1: **Resonance surfaces for the Standard Family:** $\theta \mapsto \theta + 2\pi\beta + \alpha\sin(\theta)$. **See eq. (10) for the definition of the resonance surfaces which live in the cartesian product of the phase (variable θ) and parameter (variables β and α) spaces. The projection to the (β, α) parameter plane gives the familiar "Arnold tongue" picture. Figure reproduced from McGehee and Peckham [MP 1996].**

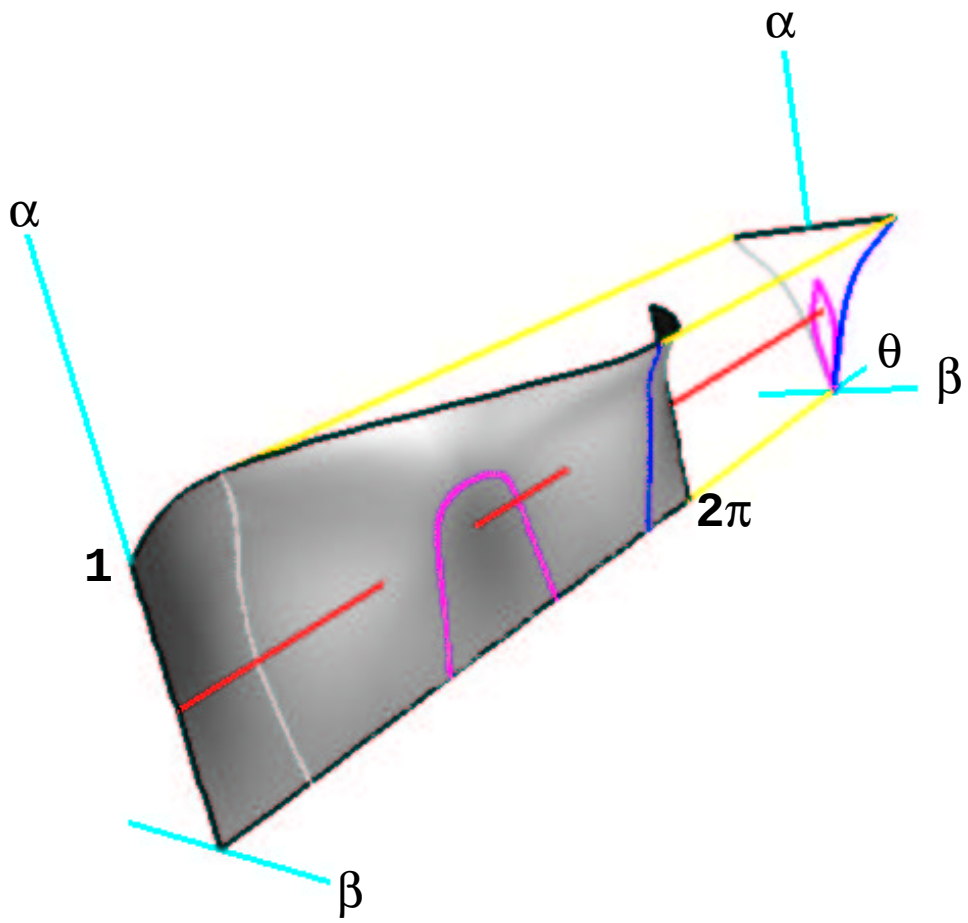

Figure 2: **An "Arnold flame" in a fixed-point resonace region for the map $\theta \mapsto \theta + 2\pi\beta + \alpha((0.1 + 0.9h(\alpha^2))\sin(\theta) + (0.9 - 0.9h(\alpha^2))\frac{\sin(2\theta)}{2}$ where $h(x)$ is a C^∞ function which increases from zero to one as x increases from zero to one. Compare with the flame for $\mathbf{F}_{(2-,\beta,\alpha)}$ in Fig. 5. Figure reproduced from McGehee and Peckham [MP 1996].**

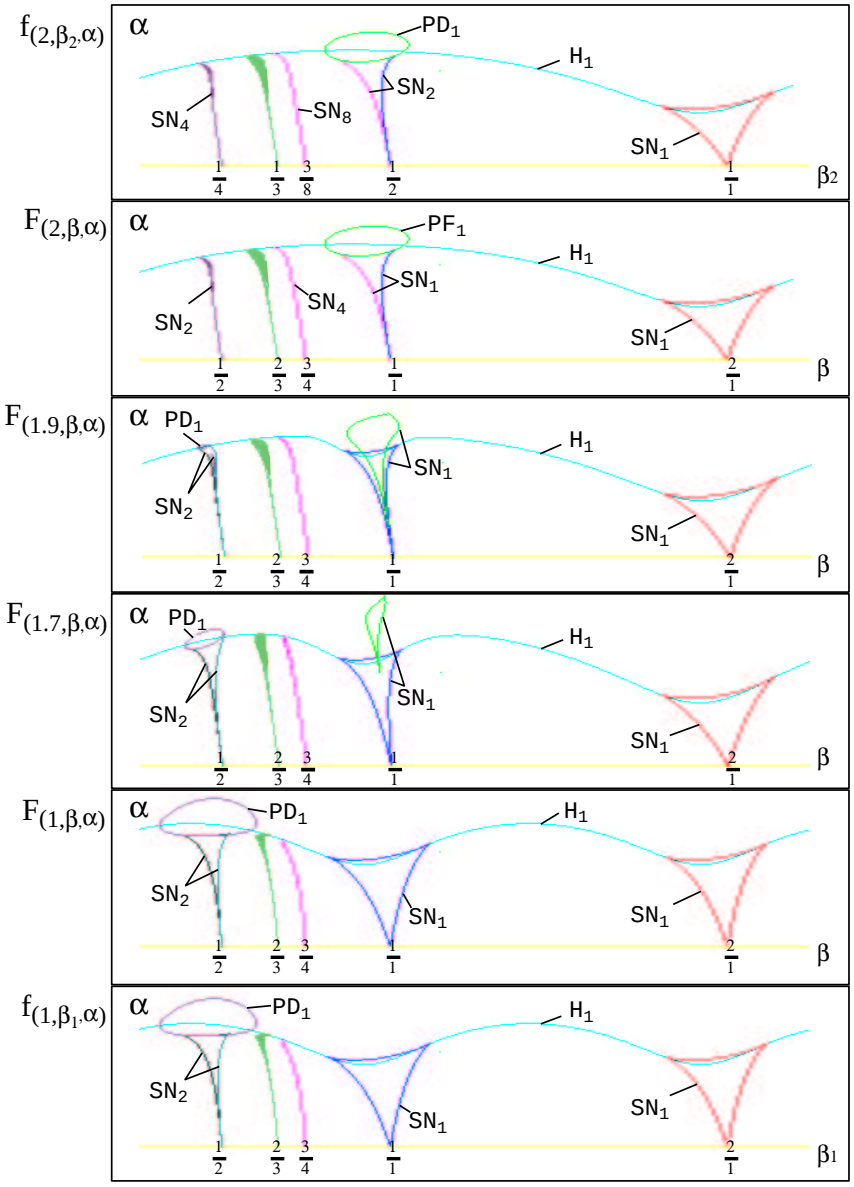

Figure 3: **Resonance region melt in the (β, α) parameter plane as a function of the relative forcing parameter γ. The (β, α) bifurcation diagram for the stroboscopic maps $\mathbf{F}_{(\gamma,\beta,\alpha)}$ ($m = 1, n = 2$ in eq. (3)) evolves from the bifurcation diagram for $\mathbf{f}_{(1,\beta_1,\alpha)}$ (without rescaling since $m = 1$) to the bifurcation diagram for $\mathbf{f}_{(2,\beta_2,\alpha)}$ (with the rescaling $\beta = 2\beta_2$) as γ increases from 1 to 2. Flames are guaranteed to exist in every p/q resonance region with p odd and γ sufficiently close to 2, and are expected to disappear for γ sufficiently close to 1. Flames are visible here in the $1/1$ region for $\gamma = 1.9$ and 1.7, and in the $1/2$ region for $\gamma = 1.9$. Abbreviations for bifurcation curves: SN: saddle-node, PD: period doubling, H: Hopf. Subscripts denote the primary period of the bifurcating orbit.**

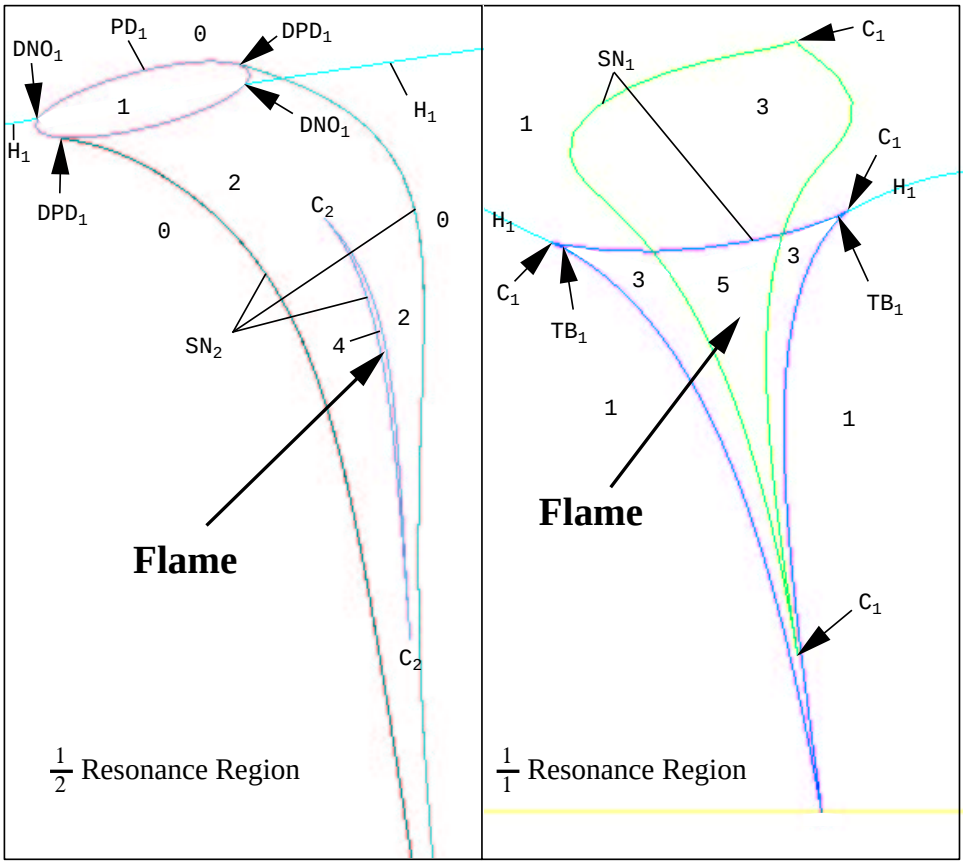

Figure 4: **Enlargement of the flames in the 1/1 and 1/2 resonance regions for $\mathbf{F}_{(1.9,\beta,\alpha)}$ in Fig. 3. The numbers indicate the number of *orbits* present for maps corresponding to parameters in each region (period-two orbits on the left, fixed points on the right). An extra pair of orbits exists for parameter values inside the flames. Abbreviations for bifurcation curves: SN: saddle-node, PD: period doubling, H: Hopf. For codimension-two bifurcation points: TB: Takens-Bogdanov (double +1 eigenvalues), DNO: Double Negative One eigenvalues, DPD: Degenerate Period Doubling (with one higher order degeneracy), C: cusp. Subscripts denote the primary period of the bifurcating orbit.**

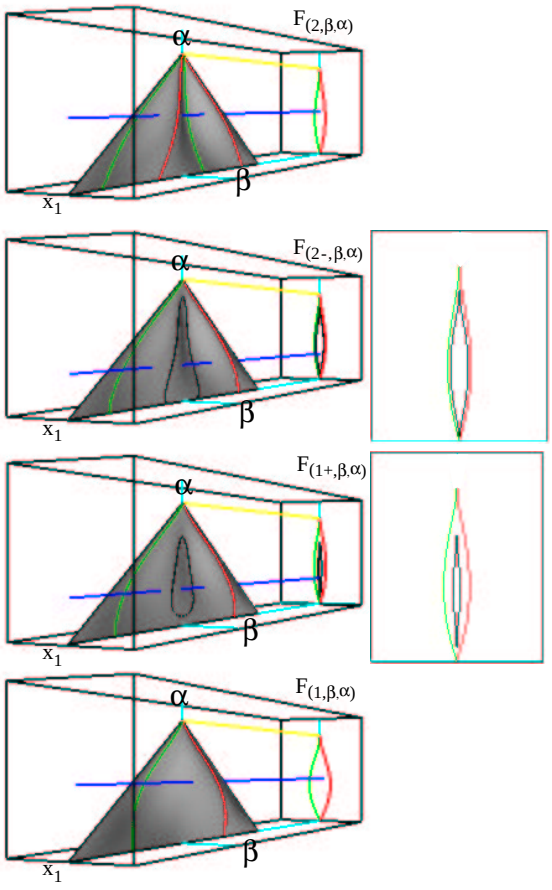

Figure 5: **Schematic $\frac{1}{5}$ resonance surface melt as a function of the relative forcing parameter γ for the stroboscopic maps of eq. (13). Projection to the (x_1, β, α) space from the four-dimensional phase $\times$ parameter space. Further projection to the parameter plane is shown on the back face of the bounding boxes. The colors of the saddle-node curves on the surfaces corresond to the colors of their projections to the parameter plane. Insets show more clearly the projection to the parameter plane of the two flames. The resonance surface evolves from the "singly folded" surface at $\gamma = 1$ to the "doubly folded" surface at $\gamma = 2$. Flames are guaranteed to exist for γ sufficiently close to 2, and are expected to disappear for γ sufficiently close to 1. See Section 2.3.1 for surface definitions, and Section 4.3 for further description.**

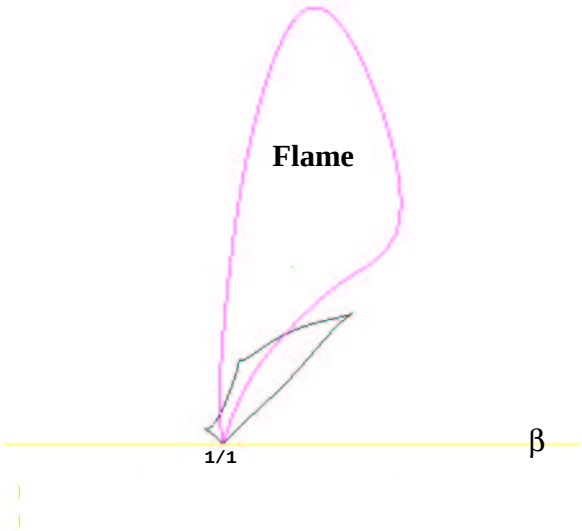

Figure 6: **Flame in the** $1/1$ **resonance region in the** (β, α) **parameter plane for the stroboscopic map of the doubly forced Brusselator of eq. (19). The relative forcing parameter** γ **is** 1.7**. This figure should be compared to the** $1/1$ **resonance region for the doubly forced caricature map,** $F_{(1.9,\beta,\alpha)}$**, in Figure 1. As in Figure 1, both curves are fixed-point saddle-node curves. As** γ **continues to decrease, the size of the flame will also decrease, disappearing entirely before** $\gamma = 1$**.**